



**HAL**  
open science

## Multispecies macrozoobenthic seasonal bioturbation effect on sediment erodibility

Amélie Lehuen, Oulhen Rose-Marie, Zhou Zhengquan, Smit Jaco De, Ijzerloo  
Lennart Van, Cozzoli Francesco, Bouma Tjeerd, Orvain Francis

► **To cite this version:**

Amélie Lehuen, Oulhen Rose-Marie, Zhou Zhengquan, Smit Jaco De, Ijzerloo Lennart Van, et al.. Multispecies macrozoobenthic seasonal bioturbation effect on sediment erodibility. 2024. hal-04608768

**HAL Id: hal-04608768**

**<https://hal.science/hal-04608768>**

Preprint submitted on 11 Jun 2024

**HAL** is a multi-disciplinary open access archive for the deposit and dissemination of scientific research documents, whether they are published or not. The documents may come from teaching and research institutions in France or abroad, or from public or private research centers.

L'archive ouverte pluridisciplinaire **HAL**, est destinée au dépôt et à la diffusion de documents scientifiques de niveau recherche, publiés ou non, émanant des établissements d'enseignement et de recherche français ou étrangers, des laboratoires publics ou privés.



Distributed under a Creative Commons Attribution - NonCommercial 4.0 International License

# MULTISPECIES MACROZOOBENTHIC SEASONAL BIOTURBATION EFFECT ON SEDIMENT ERODIBILITY

Amélie Lehuen<sup>a</sup>, Rose-Marie Oulhen, Zhengquan Zhou, Jaco de Smit, Lennart van Ijzerloo,  
Francesco Cozzoli, Tjeerd Bouma, Francis Orvain <sup>a\*</sup>

<sup>a</sup> Biologie des Organismes et Ecosystèmes Aquatiques (BOREA) Université de Caen Normandie  
UNICAEN, Sorbonne Université, MNHN, UPMC Univ Paris 06, UA, CNRS 8067, IRD, Esplanade de la  
paix, F-14032 Caen, France

\* Corresponding author: amelie.lehuen@gmail.com

## Abstract

Bioturbation in estuarine environments describes all sediment reworking processes implied in sediment transport. However, modelling at large spatial and temporal scales remains a challenge because of the need to consider the fauna at the community level, and because animal behaviour is highly seasonal. Bioturbation processes can be linked to the activity of organisms, based on the principle of energy ecology, linking the metabolic rate to the erodibility of a sediment colonised by benthic fauna. This study investigates this postulate by evaluating the erodibility parameters of a sediment subjected to: i) the bioturbation under seasonal temperature variations; ii) the joint bioturbation of different species. The experimental design consisted of: i) three temperature levels (winter, spring and summer), ii) two species combined (*Cerastoderma edule* and *Macoma balthica*; *Scrobicularia plana* and *Hediste diversicolor*; *Corophium volutator* and *Peringia ulvae*) at 4 different relative densities. Two successive experiments were carried out on the same individuals: measurement of oxygen consumption of fauna then measurement of the erodibility of the colonised sediment in a flume. The oxygen consumption confirmed that the metabolic rate is a good model of the fauna respiration, regardless of species. The erosion results indicated that the metabolic rate in the case of the fluff layer is an interesting descriptor for 1) the assessment of the bioturbation under variable temperatures and 2) the integration of the two different bioturbator species that could co-occur in the same habitat. In contrast, the effect of bioturbation on the mass erosion threshold seems to be more related to the bioturbation processes than to the metabolic rate. Bioturbation models of the fluff layer using metabolic rate is a promising tool for modelling the effects of faunal communities on sediment transport at the scale of an estuary and over the long term, even projected in the context of global warming.

## 30 Highlights

- 31 • Temperature influences the effect of bioturbation on sediment erodibility by regulating  
32 physiological metabolism.
- 33 • The erosion of the fluff layer is positively linked to the total metabolic rate, without consideration  
34 of the species.
- 35 • The mass erosion threshold is negatively impacted by some species, without consideration of  
36 their metabolic rate.

## 37 Keywords

38 Bioturbation, respirometry, erosion, erodibility, metabolic rate, intertidal, mudflat, estuaries, benthos

## 39 Manuscript

### 40 1 Introduction

41 Measuring the interaction between fauna and their environment on a large scale using generic  
42 models is necessary to better understand complex coastal and estuarine ecological systems (Carleton  
43 Ray and McCormick-Ray, 2013) and to make visible the feedback loops at work within the habitats they  
44 contain, including small-scale effects (Ettema and Wardle, 2002; Hewitt et al., 2005; Thrush et al., 2003).  
45 In particular, the impact that benthic fauna can have on sediment transport via its erodibility is an element  
46 to consider when describing the morphodynamics of an estuary. However, this impact is rarely taken  
47 into account in numerical hydro-morpho-sedimentary models [the recent work of Brückner et al is a case  
48 in point (Brückner et al., 2021)], because the fauna is considered more as an 'end user' of a habitat  
49 rather than an element in the feedback loop as a community of species interacting with each other and  
50 with the environment.

51 Indeed, many benthic species are considered to be ecosystem engineers (Jones et al., 1994), and  
52 play a crucial role in the formation, transformation and maintenance of habitats. Bioturbation covers all  
53 the mechanical and biological processes by which ecosystem engineers can modify sediment and its  
54 erodibility. This includes actions such as digging galleries, stirring up sediments and mixing sediment  
55 layers (Jones et al., 1997; Kristensen et al., 2012; Le Hir et al., 2007; Meysman et al., 2006). Historically,  
56 studies of the effects of bioturbation on sediment erodibility have been carried out for isolated species  
57 and the best proxy was defined by the density or biomass of the species at the time of measurement.

58 The species chosen are generally frequently found in intertidal areas, such as *Macoma balthica*  
59 (Paarlberg et al., 2005; Widdows and Brinsley, 2002; Widdows et al., 2000), *Cerastoderma edule*  
60 (Andersen et al., 2010; Dairain et al., 2020a, 2020b; Li et al., 2017; Rakotomalala et al., 2015; Widdows  
61 et al., 1998), *Hediste diversicolor* (de Deckere et al., 2001), *Scrobicularia plana* (Kristensen et al., 2013;  
62 Orvain, 2005; Soares and Sobral, 2009), *Peringia ulvae* (Andersen et al., 2005, 2002; Orvain et al.,  
63 2003), *Corophium volutator* (de Deckere et al., 2000).

64 To describe the effects of bioturbation on the scale of an estuary-type environment over the long  
65 term, it is necessary to consider a community of species rather than isolated species, and to take  
66 account of the seasonal variation in species activities. It is therefore necessary to use a biological  
67 descriptor that is adapted to the physiological or functional diversity of the species while reflecting the  
68 seasonal cycles in order to describe the bioturbation mechanisms involving different species over time.

69 Based on the principle that bioturbation is the result of an individual's activity as much as its  
70 morphology and physiological state, and that this activity requires energy which results from its  
71 metabolism, the sum of the metabolisms of a population, or even a community, appears to be a relevant  
72 indicator for assessing the effects of bioturbation on sediment erodibility. According to Brown's definition,  
73 "metabolism is the biological processing of energy and materials" (Brown et al., 2004). For heterotrophic  
74 organisms, the metabolic rate is assimilated to respiration, the basis of their energy transformation  
75 (Brown et al., 2004).

76 The metabolic rate has been modelled as the Standard Metabolic Rate, which varies as a function  
77 of body mass and temperature (Allen et al., 2005; Brey, 2010). Although the rigid mechanistic  
78 interpretation of individual energy scaling laws and their larger-scale effects by the metabolic theory of  
79 ecology (MTE) is widely debated and partly overcome (Glazier, 2022), the increase in metabolic rates  
80 with size and temperature remains one of the fundamental general trends observed in living things.  
81 Metabolic theories are therefore widely used as a mechanistic basis for models of ecological dynamics  
82 at all scale levels (Posfai et al., 2017). The dependence of metabolic rates on temperature makes these  
83 models particularly useful in terms of predicting the functioning of ecosystems subject to seasonal  
84 variations but also potentially under the effect of global warming (Huey and Kingsolver, 2019).

85 Studies have explored the possibility of defining the effects of bioturbation of isolated species on  
86 sediment erodibility using the energy balance rather than the traditional descriptors of biomass, density  
87 or size of individuals (Cozzoli et al., 2018). The energy approach proposes the use of metabolic rate,  
88 i.e. the amount of energy expended by an organism for its survival, as a parameter to model bioturbation  
89 effects in an environmental energy balance (Cozzoli et al., 2021; Lehuen and Orvain, 2024).

90 An attempt at multi-species modelling describing facilitated erosion of the biogenic matrix was made  
91 by integrating such "metabolic respiration rate" (Cozzoli et al., 2019). Even though this approach was  
92 performed for several bioturbators, calculations were only applied to separate single-species datasets  
93 until now. Another study mixed some benthic species, but only the erosional effects of the sediment

94 structural layer were described (de Smit et al., 2021a). Because of the number of interactions that may  
95 exist between species, the effects of species may vary according to their behavioural functions. All these  
96 effects may therefore add up, cancel each other out or not affect the same factors, depending on their  
97 nature or the nature of the interactions between the species themselves.

98 In this study, we propose to explore these various aspects in a multifactorial protocol. Firstly, we use  
99 metabolic rate as a biological descriptor of fauna to explain the effects of bioturbation from an energetic  
100 point of view, by measuring the respiration rate of the individuals used to check the suitability of the  
101 SMR model. Secondly, we take into account the variability of faunal activity as a function of temperature  
102 and its impact on the effects of bioturbation on sediment erodibility, by exposing individuals on sediment  
103 to three temperature levels corresponding to the seasonal cycle during a period of bioturbation before  
104 measuring erodibility. Thirdly, we measure the effects of bioturbation on sediment erodibility of several  
105 species combined in the same sediment simultaneously, and at different relative densities, in order to  
106 assess the impact of interactions between species on bioturbation. These species were paired according  
107 to their functional groups to study various cases of interactions.

## 108 2 Material and Methods

### 109 2.1 Biological models

110 The species selected were based on the communities observed in intertidal areas of estuaries in  
111 north Atlantic, such as the Seine estuary or Schelde estuary, choosing the more frequent and ubiquitous  
112 ones (Figure 1A). This study proposes to evaluate combined bioturbation effects of those six emblematic  
113 species by defining three species duos to explore the following questions (Figure 1B):

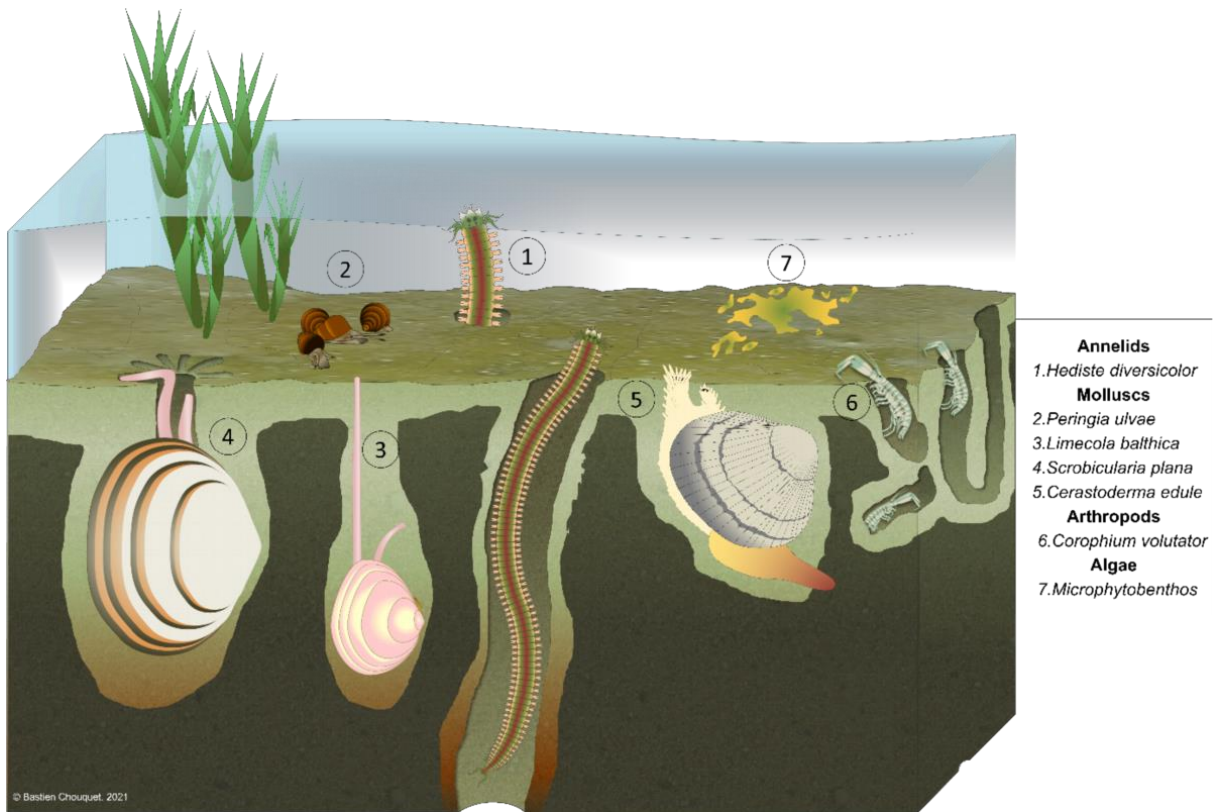
- 114 1. *Cerastoderma edule* and *Macoma balthica*: do these two species that look alike have same  
115 bioturbation effect, even though they do not have the same feeding behaviour? They both  
116 create a biogenic layer on the first few centimetres of sediment and can play a role in both  
117 types of erosion (fluff and mass erosion). However, *C. edule* is strictly a suspension feeder,  
118 whereas *M. balthica* is a mixed suspension and deposit feeder at low tide, influencing the  
119 water-sediment interface more directly. The two species are known to facilitate each other  
120 and cohabit (Bocher et al., 2007; Montserrat et al., 2009; Ysebaert et al., 2003) and are cited  
121 together to describe communities in the EUNIS habitat A2.24 : Polychaete/bivalve-  
122 dominated muddy sand shores (A2.241/MA5251, A2.242/MA5252, A2.243/MA5253) and  
123 A2.31 : Polychaete/bivalve-dominated mid estuarine mud shores (A2.312/MA6224,  
124 A2.313/MA6225) (European Environment Agency, 2023).
- 125 2. *Scrobicularia plana* and *Hediste diversicolor*: The question is “does the cohabitation of species  
126 mitigate antagonistic bioturbation effects?”. Those two species are known for their  
127 antagonistic effects on the deep structure of the sediment: *H. diversicolor* is a biostabilizator,

128 *S. plana* is a bed destabilizer. These antagonistic effects were observed *in situ* during  
129 experiments carried out on enclosures enriched with one or the other species, after one week  
130 under winter conditions and at the end of summer (Morelle et al., 2024). They also both  
131 create traces on the sediment surface (bioresuspension), but *S. plana* also generates  
132 pseudo-faeces when filtrating water (biodeposition). By definition, this duo is the least  
133 suitable for unifying a model without taking into account the bioturbation functional group.  
134 They live and often co-exist in mud or sandy-mud, frequently anoxic under 1 cm depth  
135 (EUNIS habitat A2.313/MA6225).

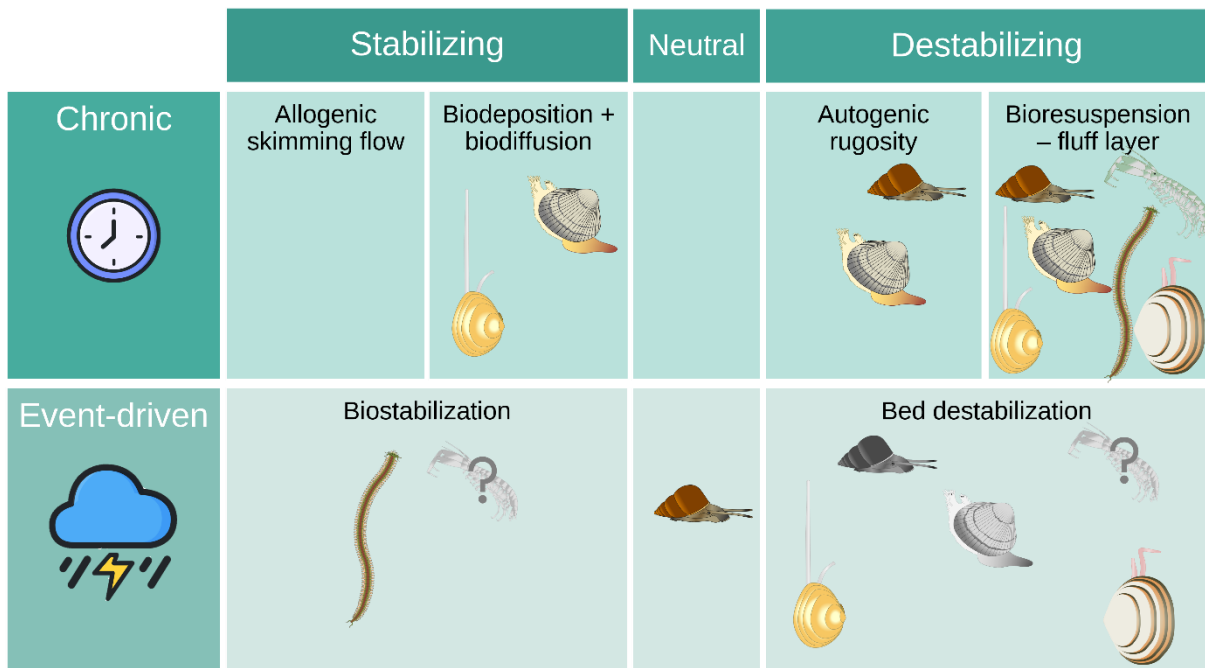
136 3. *Corophium volutator* and *Peringia ulvae*: can the effect of two surface-mobile deposit feeders  
137 on erosion parameters be equated? *C. volutator* and *P. ulvae* have similar influence on a  
138 very fine upper layer by crawling over the sediment-water interface for capturing  
139 microphytobenthic biofilms. They can be found in the same type of habitats, sheltered  
140 estuaries with muddy-sand or sandy-mud sediment, classified EUNIS A2.243/MA5253 and  
141 A2.312/MA6224.

142 Based on the theoretical frame of Brown and Allen (Allen et al., 2005; Brown et al., 2004), the  
143 individual metabolic rate  $I$  was expressed as function of the individual body size ( $M$ ) and the temperature  
144 ( $T$ ):  $I \approx r_0 M^b \cdot e^{-E_k/T}$ . The equation was adjusted the parameters  $r_0$ ,  $b$  and  $E_k$  for each species to the Standard  
145 Metabolic Rate (SMR) of aquatic invertebrates model of Brey (Brey et al., 2010).  $I_{tot}$  [ $\text{mW}\cdot\text{m}^{-2}$ ] is thus  
146 the sum of basal metabolic rate of all individuals in the sample (details in Supplementary data 2.1).

A



B



147 Figure 1 A: Fauna models used in their sediment. B: Classification of species according to the  
 148 different effects of bioturbation on sediment characteristics (references in Supplementary data 2.1,  
 149 SuppFig 2.B and SuppTab 2.C).

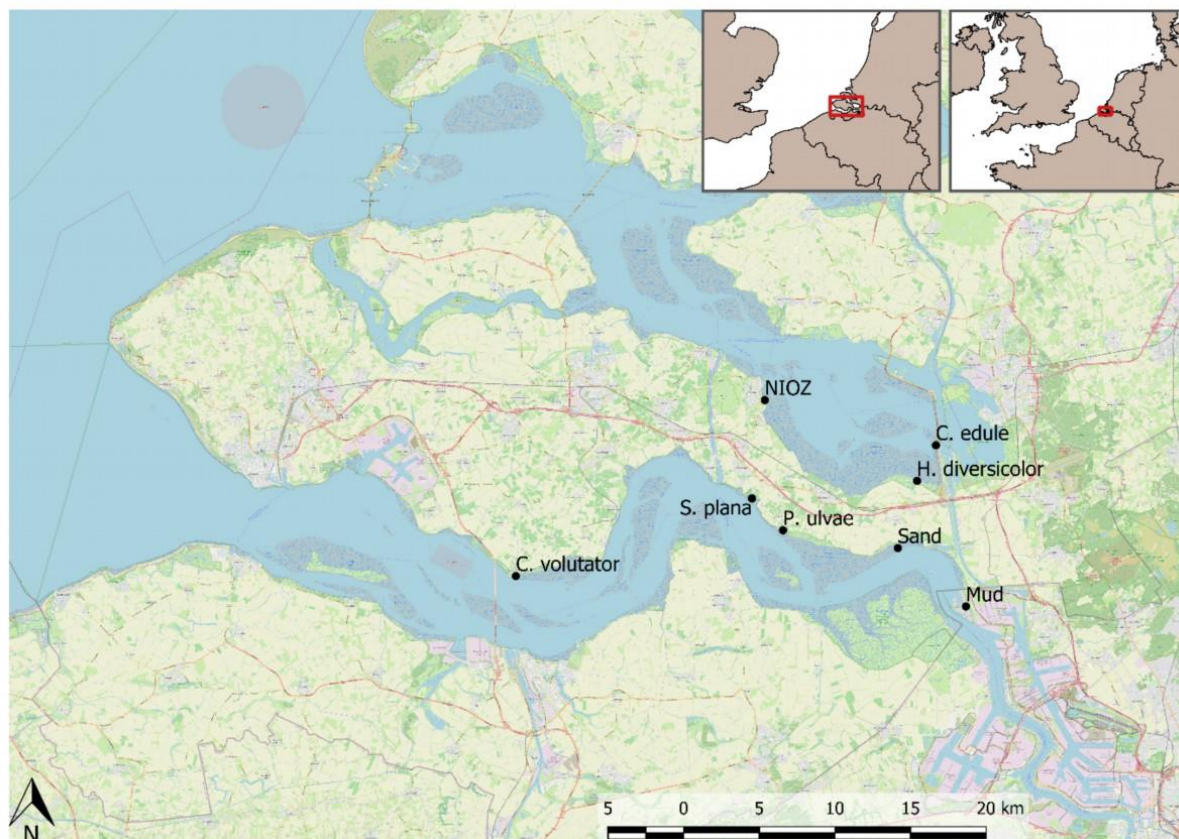
## 150 2.2 Sediment and animal collection

151 The Schelde estuary, a macrotidal coastal estuary, situated between The Netherlands and Belgium,  
152 is split in two main parts, named Westerschelde (south part) and Oosterschelde (north part). Due to  
153 anthropological transformations, the Oosterschelde is no longer fed by Schelde freshwater (Louters et  
154 al., 1998) (Figure 2).

155 A muddy and a sandy sediment were collected in the Westerschelde (mud in Groot Buitenschoor  
156 D50 = 20.69  $\mu\text{m}$ ; silt fraction 85.79 % < 63  $\mu\text{m}$ ; sand in Rilland D50 = 158.83  $\mu\text{m}$ ; silt fraction 3.53 % <  
157 63  $\mu\text{m}$ ), wet-sieved at 5mm and defauned 48h in a freezer, then wet-sieved at 1mm to remove fauna  
158 and larger debris. Each sediment grain-size profile was characterized with a Mastersizer 2000 (Malvern  
159 Instruments Ltd., Malvern, UK). A 50%-50% vol mix was made (D50 = 67.99  $\pm$  14.17  $\mu\text{m}$ ; silt fraction  
160 48.81  $\pm$  3.21 % < 63  $\mu\text{m}$ ), and let settle for two weeks to reduce the water content (33.30 %  $\pm$  0.78 %).  
161 The water content, density, grain-size composition and organic matter were monitored all along the  
162 experiment (details of sediment characteristics in Supplementary data 2.2 SuppFig 2.E, SuppTab 2.D).

163 Species were collected either in Oosterschelde or Westerschelde; *C. edule* in Oesterdam and in Den  
164 Inkel; *H. diversicolor* in Haven Rattekaai; *C. volutator* in Haventje Ellewoutsdijk; *S. plana* and *M. balthica*  
165 in Den Inkel; *P. ulvae* in Nolleweg. Individuals of each species were sorted to create batches of size  
166 classes, and a sub-sample of each class were used to measure length, fresh weight, dry weight, Ash  
167 Free Dry Weight (gAFDW) and define conversion coefficients that were used to define sample  
168 populations experiment (results in Supplementary data 2.2). The rest of the individuals were placed in  
169 the acclimatized mesocosms (thermoregulation).





170

171 *Figure 2 Maps of sampling location for each species and sediment.*

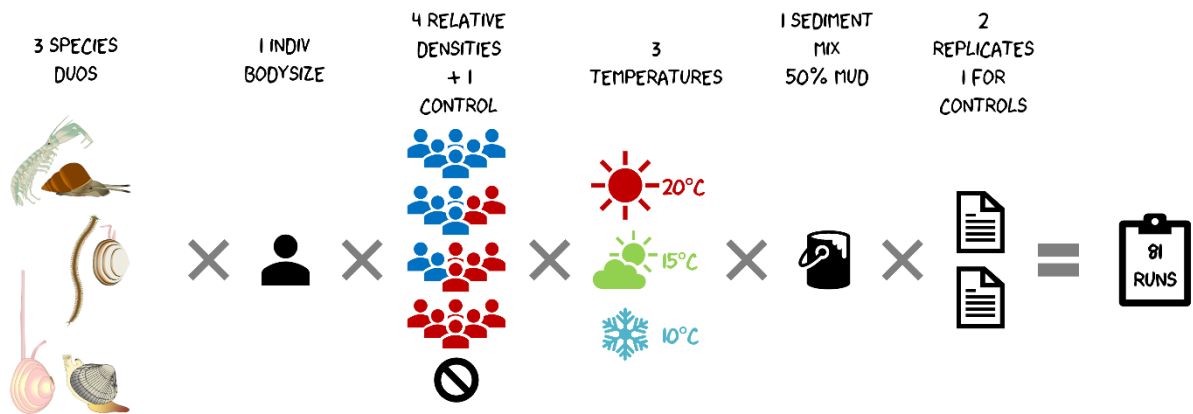
## 172 2.3 Experimental design

173 The design of the experiment was built to measure the erodibility properties of the sediment for  
 174 combined species and at varying temperatures (Figure 3A). Biological samples consisted in 3 duos of  
 175 species of fixed body size, with 4 levels of relative densities for a global stable metabolic rate and a  
 176 control. Experiments were run at three levels of temperatures that would represent winter, spring and  
 177 summer (setpoint 10, 15, 20°C) (details in Supplementary data 2.4 SuppTab 2.E and SuppFig 2.L, M).  
 178 Two replicates were made for each condition.

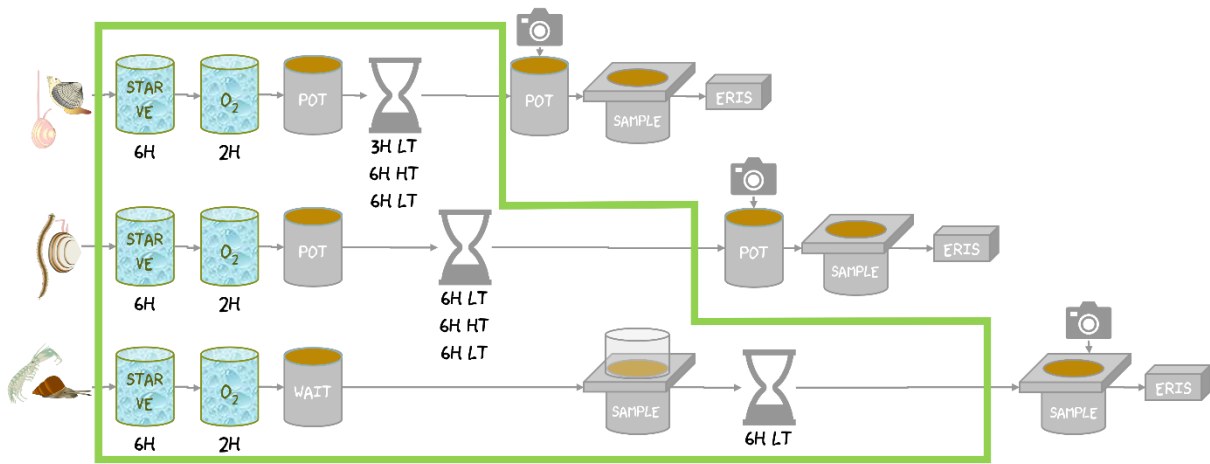
179 Measurement started with a respiration measurement of the biological samples in filtered sea water  
 180 (salinity 31) at control temperature. Then fauna samples were settled in an incubation core of muddy  
 181 sediment with a smoothed surface in a mesocosm under a tidal rhythm (Figure 3C) with controlled  
 182 temperature for a bioturbation period. The colonized sediment cores were then used in an erosion  
 183 measurement in flume, made with filtered sea water at room temperature.

184 Depending on the erosion measurement sequence (3 hours of measurement and cleaning with one  
 185 flume, Figure 3B), the bioturbation duration varied from 6h to 18h, with an adapted set-up for *Corophium*  
 186 *volutator* and *Peringia ulvae*, to ensure their presence on the sample bearer. The fauna was in this case  
 187 put in a waiting mesocosm, and installed directly on the sample bearer for bioturbation, resulting to the  
 188 absence of seawater during the bioturbation period (Figure 3C).

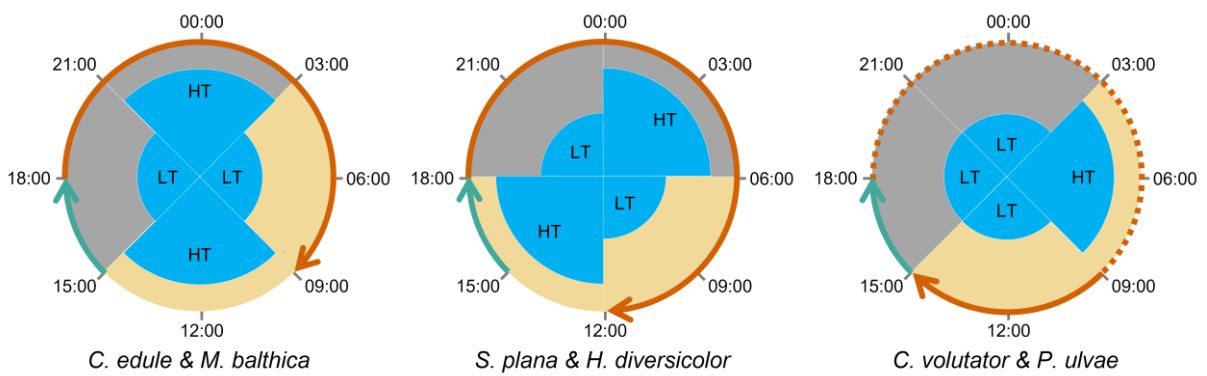
A



B



C



189 Figure 3 A: Experimental design. B: Measurement's chronology. LT: low tide, HT: high tide, O<sub>2</sub>:  
 190 respiration chamber, pot: incubation core, sample: sample bearer for the erosion flume, ERIS: erosion  
 191 flume. The green frame represents the steps with a controlled temperature. C: Mesocosms tidal rhythm  
 192 for each duo. The blue arrow represents the respiration measurement and the installation in the pot, the  
 193 red arrow the bioturbation phase, the red dotted line the holding period of *C. volutator* and *P. ulvae* in a  
 194 dedicated mesocosm prior to installation on sample bearer.

## 195 2.4 Experimental measurements

### 196 2.4.1 Respiration measurements

197 Selected animals for each sample were individually weighted or measured then put in filtered sea  
198 water for 6h to starve, in order to reduce metabolic consumption due to digestion and O<sub>2</sub> side  
199 consumption by faeces. The sample pools were then placed in a hermetic respiration chamber (V =  
200 1.5L) with stirring. The oxygen concentration [ $\mu\text{mol.L}^{-1}$ ] was measured during 2h using a PyroScience  
201 FireStingO2 sensor, without light nor human presence. In the measurement sequence, 3 periods visually  
202 without disturbance were selected to calculate 3 slopes of a linear regression, summarized as mean  
203 and standard deviation as the respiration rate [ $\mu\text{molO}_2.\text{s}^{-1}$ ]. Based on (Brey et al., 2010) the respiration  
204 rate was converted into metabolic rate  $Itot_{respi}$  [mW] with the oxycalorimetric coefficient 468 J/mmolO<sub>2</sub>,  
205 and divided by the surface of the flume for consistency [ $\text{mW.m}^{-2}$ ].

206 The mean respiration chamber temperature was used to calculate a mesocosm metabolic rate  
207  $Itot_{meso}$  for the sample surface of flume [ $\text{mW.m}^{-2}$ ]. In addition, given the water temperature was not  
208 controlled during the flume experiment, the mean water temperature in the flume was used to calculate  
209 a flume  $Itot_{flume}$  [ $\text{mW.m}^{-2}$ ]. When  $Itot$  is mentioned, the same treatment was made with the three metabolic  
210 rates.

### 211 2.4.2 Sediment erodibility analyses

212 ERIS is a unidirectional flume designed by Ifremer to measure the erodibility of non-cohesive and  
213 cohesive sediments. The mass erosion threshold and the erosion flux are calculated from the turbidity  
214 in response to increasing shear stress. The shear stress is modulated by different flow velocities in a  
215 closed channel. Details about flume set up are in (Guizien et al., 2012; Le Hir et al., 2008; Orvain et al.,  
216 2014b). Erosion experiment run by steps with current velocity from 0 to 91  $\text{cm.s}^{-1}$  in 14 steps lasting 5  
217 to 8 min, for a total of 2 hours measurement. The bed shear stress ( $BSS$  or  $\tau$  [Pa]) was converted from  
218 the current velocity based on (Guizien et al., 2012), without accounting for sediment bed roughness,  
219 and turbidity measurement was converted into resuspended mass calculated on the sample surface,  
220  $M_{erod}$  [ $\text{g.m}^{-2}$ ]. Every current step was defined, and fluff or mass erosion steps were identified visually.  
221 Every step was summarized with mean of hydrological conditions, and the 95<sup>th</sup> centile of the  $M_{erod}$ . The  
222 critical  $BSS_{mass}$  [Pa] was calculated as the value of the  $BSS$  corresponding to  $M_{erod} = 0$  on the linear  
223 regression on the mass steps. The  $Q_{fluff}$  was determined as the 95<sup>th</sup> centile of  $M_{erod}$  at the last fluff erosion  
224 step before mass erosion was visible (details in Supplementary data 2.4 SuppFig 2.N).

### 225 2.4.3 Data analysis

226 Respiration measurement results were compared to the metabolic rate  $Itot_{meso}$  calculated with the  
227 mesocosm temperature. Both variables were normalized with a Box-cox transformation (function

228 `AID::boxcoxnc`, with  $y = (x+\lambda_2)^\lambda/\lambda$ , and a correlation was calculated to assess the adequacy of the  
229 Brey model to account for fauna activity. An one-way ANCOVA was made with the metabolic rate based  
230 on respiration measurement as dependant variable and  $Itot_{meso}$  as covariate, with two factors: 1) duos  
231 to ensure experimental conditions does not create differences between species; 2) temperature  
232 conditions that reflect also the global sequence of experiments (details in Supplementary data 2.4  
233 SuppFig 2.I).

234 Both bioturbation parameter  $Q_{fluff}$  and erosion parameter  $BSS_{mass}$  were normalized with a Box-Cox  
235 transformation and used as dependant variable in a one-way ANCOVA with the metabolic rate ( $Itot_{meso}$ )  
236 as covariate, and temperature or duos as factor to assess the species dependency of erosion  
237 parameters to the general metabolic rate. A linear regression of each transformed erosion parameter  
238 was conducted regarding the metabolic rate of the two species in the duos separated to evaluate their  
239 relative bioturbation role.

240 The validity of ANCOVAs were verified by evaluating the normality of the sub-groups per factors, the  
241 independence of covariant and factors was tested with ANOVA and the homogeneity of regression  
242 slopes for each sub-group was checked. Post-hoc tests were made for testing validity conditions  
243 (homogeneity of variance, normality and homoskedasticity of residues, outliers). Models and post hoc  
244 tests were conducted with packages `broom` (`tidy`, `glance`, `augment` (Robinson et al., 2023)),  
245 `performance` (`compare_performance` (Lüdecke et al., 2021)), `rstatix` (Shapiro-Wilk, Levene,  
246 ANOVA & ANCOVA (Kassambara, 2023)), `lmttest` (Harrison-McCabe test) and `emmeans` (Estimated  
247 marginal means of linear trends (Lenth et al., 2023)). All data processing was conducted in R version  
248 4.3.0.

## 249 3 Results

### 250 3.1 Respiration measurements

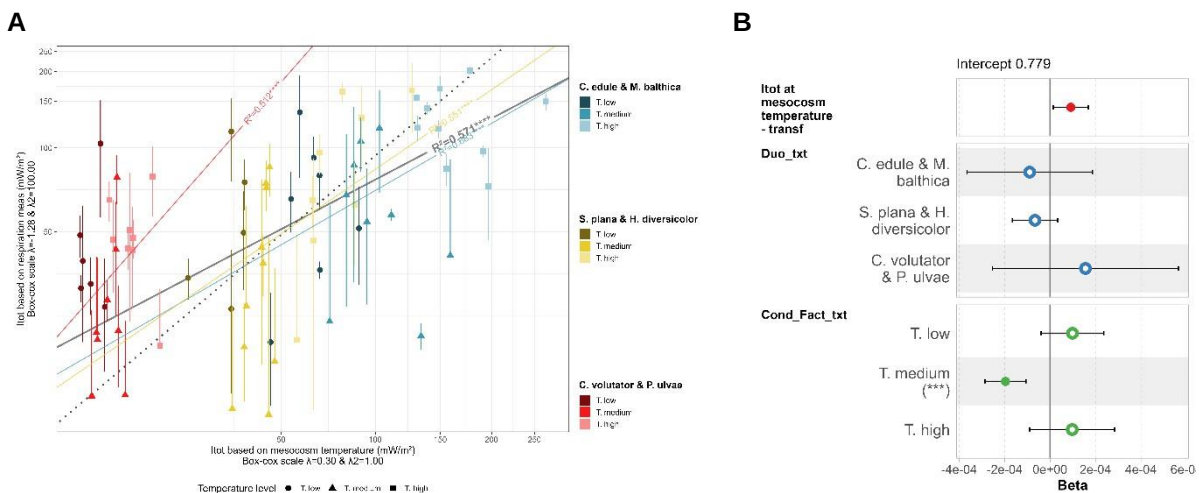
251 The overall oxygen consumption was measured for *C. edule* & *M. balthica* at  $0.0012\pm 0.0007$   
252  $\mu\text{molO}_2\cdot\text{s}^{-1}$  ( $n = 27$ ), *S. plana* & *H. diversicolor* at  $0.0008\pm 0.0006$   $\mu\text{molO}_2\cdot\text{s}^{-1}$  ( $n = 26$ ) and *C. volutator* &  
253 *P. ulvae* at  $0.0004\pm 0.0004$   $\mu\text{molO}_2\cdot\text{s}^{-1}$  ( $n = 27$ ), corresponding to respectively  $0.03\pm 0.02 \times 10^{-4}$   $\mu\text{molO}_2\cdot\text{s}^{-1}$ .gAFDW<sup>-1</sup>;  
254  $0.06\pm 0.04 \times 10^{-4}$   $\mu\text{molO}_2\cdot\text{s}^{-1}$ .gAFDW<sup>-1</sup> and  $0.28\pm 0.33 \times 10^{-4}$   $\mu\text{molO}_2\cdot\text{s}^{-1}$ .gAFDW<sup>-1</sup>, and  $88\pm 50$ ;  
255  $55\pm 44$  and  $27\pm 31$  mW.m<sup>-2</sup> (details in Supplementary data 3.1 SuppTab 3.A). The metabolic rate based  
256 on respiration rate measurements,  $Itot_{respi}$ , was normalized with a Box-Cox transformation ( $\lambda = -1.280$   
257 and  $\lambda_2 = 100$ ), as well as  $Itot_{meso}$  calculated at the mesocosm temperature ( $\lambda = 0.3$  and  $\lambda_2 = 1$ ).

258 The metabolic rate  $Itot_{respi}$  [mW.m<sup>-2</sup>] was plotted against the modelled  $Itot_{meso}$  (Figure 4A). The dataset  
259 with *C. volutator* & *P. ulvae* showed correlation between  $Itot_{meso}$  calculated and the measured  $Itot_{respi}$  ( $R^2 = 0.512^{****}$ )  
260 with a slope significantly different than the two other duos, *C. edule* & *M. balthica* ( $R^2 = 0.683^{****}$ )  
261 and *S. plana* & *H. diversicolor* ( $R^2 = 0.551^{****}$ ). The global regression was considered

262 representative enough of the global link between the two variables ( $R^2 = 0.571^{****}$ ). The global slope,  
 263 like that of *C. edule* & *M. balthica* and *S. plana* & *H. diversicolor*, had a value slightly below the identity  
 264 line (i.e. the diagonal), but with a higher intercept, meaning that a low  $Itot_{meso}$  underestimates  $Itot_{respi}$ ,  
 265 while a high  $Itot_{meso}$  overestimates it. For *C. volutator* & *P. ulvae*,  $Itot_{meso}$  systematically underestimates  
 266  $Itot_{respi}$ , meaning that the individuals were more active than expected.

267 The ANCOVA results of  $Itot_{respi}$  transformed  $\sim Itot_{meso}$  transformed + Duo + Temperature ( $F_{(2,65)} =$   
 268 6.64,  $p = 0.002$ , Figure 4B, details in Supplementary data 3.1 SuppTab 3.B, C) show that there was no  
 269 significant effect of the duos on  $Itot_{respi}$  but a significant effect of the temperature, in particular the medium  
 270 temperature that would lead to a lower  $Itot_{respi}$  value.

271 Note that for all the ANCOVAs performed in the study, the  $Itot_{meso}$  covariate has a significant  
 272 relationship with the factors, either duos or temperature, as these factors are used to define  $Itot_{meso}$ . The  
 273 violation of this hypothesis is accepted because of its very nature:  $Itot_{meso}$  is defined independently of  
 274 any measurement, the ANCOVA results would then indicate whether duos & or temperature have  
 275 additional effects to those expected and taken into account by  $Itot_{meso}$  (metabolism more active than  
 276 basal for example).



277 Figure 4 A:  $Itot_{respi}$  [ $mW \cdot m^{-2}$ ] vs  $Itot_{meso}$ , with standard deviation and its regression line for each duo  
 278 (corresponding colours) and in grey for all data combined, the grey dotted line represents the identity  
 279 relation. Note that the scales are Box-Cox transformed, and the regression lines were made on  
 280 transformed data. B: ANCOVA results for  $Itot_{respi}$  transformed  $\sim Itot_{meso}$  transformed + Duo +  
 281 Temperature. Filled dot are  $p$ -value  $\leq 0.1$  and empty dot are  $p$ -value  $> 0.1$ .

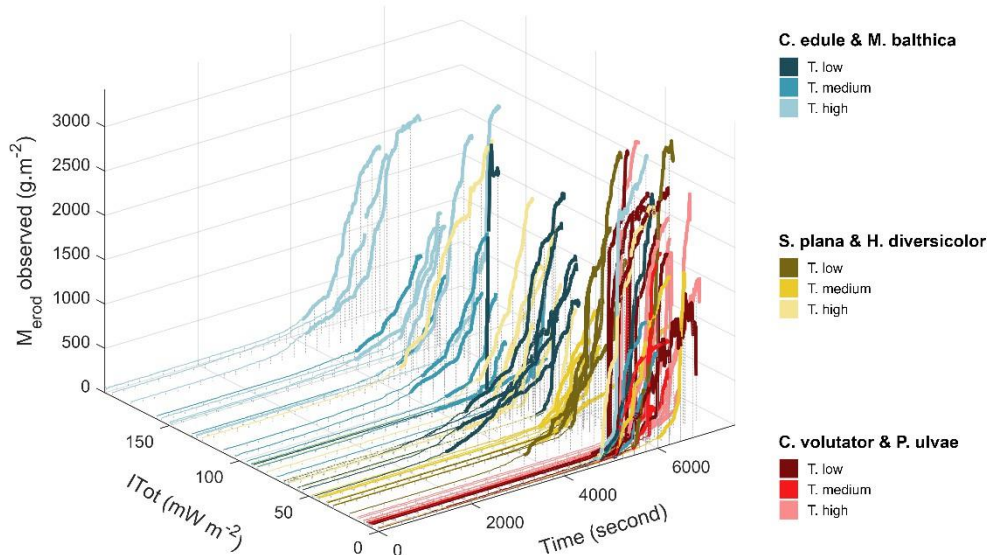
## 282 3.2 Erodibility analysis

### 283 3.2.1 Erosion data treatment

284 All erosion runs made on ERIS flume were treated similarly to determine when the fluff layer erosion  
 285 and mass erosion occurred (Figure 5). Fluff layer erosions were observed mainly from the seventh to  
 286 the eleventh step of bed shear stress  $BSS = 0.81 \pm 0.53$  Pa corresponding the shear velocity  $U^* =$   
 287  $2.67 \pm 0.87$   $cm \cdot s^{-1}$ . Mass erosion occurred mainly between the eleventh and the fourteenth steps of bed

288 shear stress BSS =  $1.73 \pm 0.74$  Pa, i.e. a shear velocity of  $U^* = 4.01 \pm 0.87$  cm.s<sup>-1</sup> (details in Supplementary  
289 data 3.2.1 SuppTab 3.D).

290 The temperature of the water in the flume was significantly higher than in the mesocosm, leading to  
291 a  $Itot_{flume}$  systematically higher than the  $Itot_{meso}$  (details in Supplementary data 2.4 SuppTab 2.E and  
292 SuppFig 2.L). For the erosion results, the three ways of calculation of metabolic rate were examined.



293

294 *Figure 5 Erosion  $M_{erod}$  ( $g.m^{-2}$ ) vs time (s) and mesocosm metabolic rate ( $Itot_{meso}$  [ $mW.m^{-2}$ ]). The thick*  
295 *solid lines represent the steps identified as mass erosion steps. The various colours represent the*  
296 *different combination of species and temperature.*

### 297 3.2.2 Fluff layer erosion

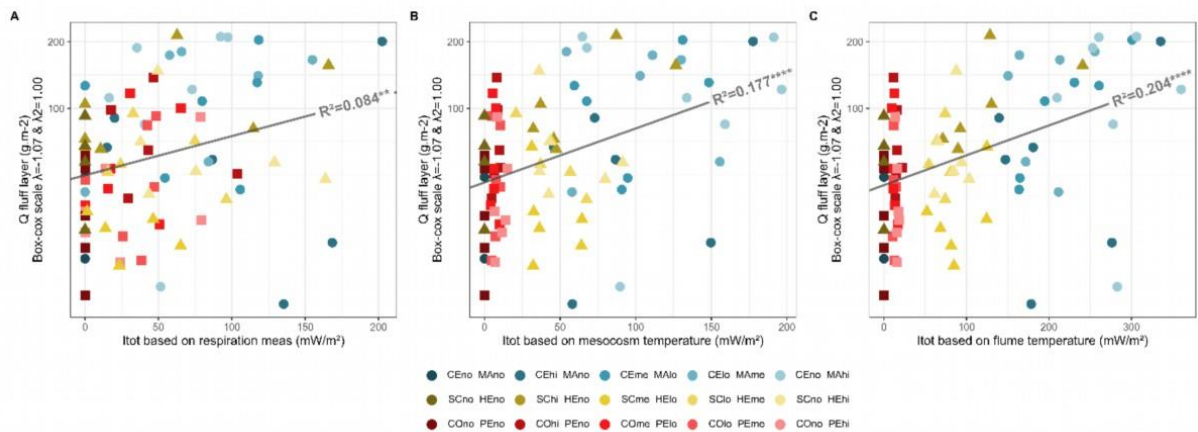
298 The estimated fluff layer quantity ( $Q_{fluff}$  [ $g.m^{-2}$ ]) showed a high dispersion in regard of any of the three  
299 metabolic rate of the sample (Figure 6).  $Q_{fluff}$  was measured for controls at  $66 \pm 14$   $g.m^{-2}$  ( $n = 14$ ), *C.*  
300 *edule & M. balthica* at  $118 \pm 57$   $g.m^{-2}$  ( $n = 25$ ), *S. plana & H. diversicolor* at  $84 \pm 39$   $g.m^{-2}$  ( $n = 23$ ) and  
301 *C. volutator & P. ulvae* at  $73 \pm 22$   $g.m^{-2}$  ( $n = 24$ ).  $Q_{fluff}$  was normalized by a Box-Cox transformation ( $\lambda =$   
302  $-1.07$  and  $\lambda_2 = 100$ ).

303 A linear model of transformed  $Q_{fluff}$  versus  $Itot$  showed a low value of indicator  $R^2$ , the  $Itot_{flume}$  being  
304 with the best ( $R^2 = 0.204^{****}$ ), followed by  $Itot_{meso}$  ( $R^2 = 0.177^{****}$ ),  $Itot_{respi}$  ( $R^2 = 0.084^{**}$ ) being the lowest  
305 (Figure 6). An ANCOVA was conducted on  $Q_{fluff}$  transformed as a dependent variable, with  $Itot_{meso}$  as  
306 covariant and temperature as factor ( $F_{(2,82)} = 0.21$ ,  $p = 0.8$ , Figure 7-A1, details in Supplementary data  
307 3.2.2 SuppTab 3.E, H). There was no significant effect of duos but a significant effect of the metabolic  
308 rate ( $p < 0.1$ ). The positive value of the global slope indicates that the higher the metabolic rate, the more  
309 fluff layer is created and resuspended.

310 An ANCOVA was conducted on  $Q_{fluff}$  transformed as dependent variable, with  $Itot_{meso}$  as covariant  
311 and duos as factor ( $F_{(3,81)} = 0.22$ ,  $p = 0.88$ , Figure 7-A2, details in Supplementary data 3.2.2 SuppTab

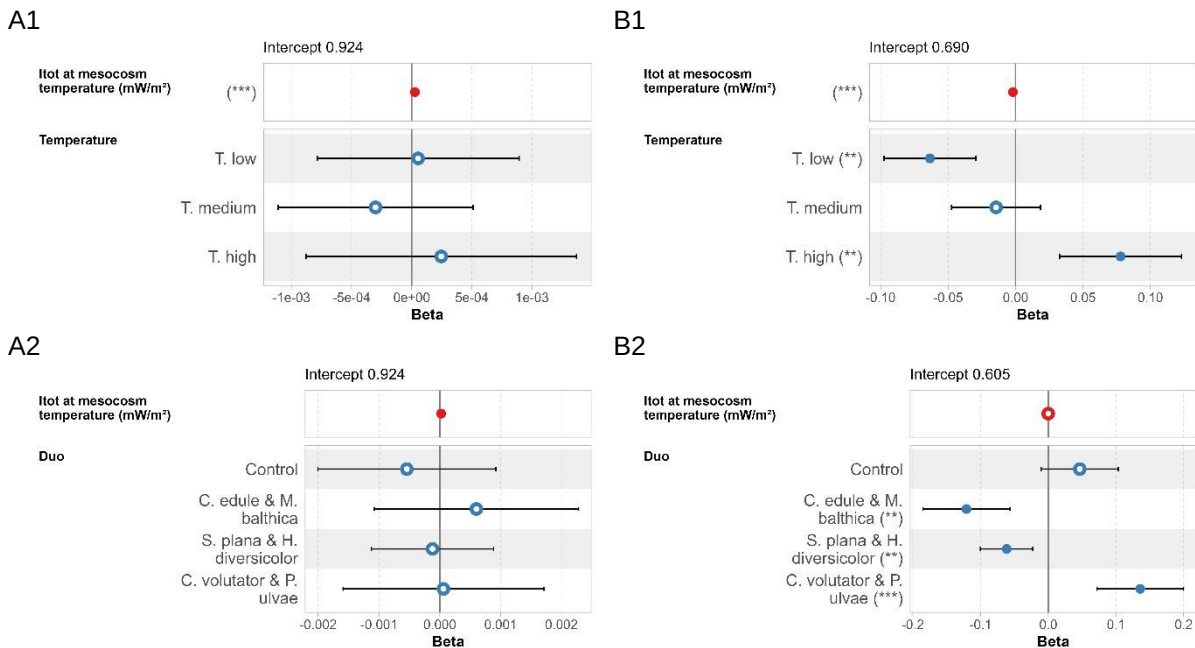
312 3.F, H). There was no significant effect of duos but a significant effect of the metabolic rate ( $p < 0.1$ ). The  
 313 positive value of the global slope indicates that the higher the metabolic rate, the more fluff layer is  
 314 created and resuspended.

315 A linear regression of  $Q_{fluff}$  as a function of the two metabolic rates of each species within duos has  
 316 an  $R^2$  similar to overall  $Itot_{meso}$  ( $R^2 = 0.177^{***}$ ,  $n = 86$ , Table 1). The slopes for the two species are similar  
 317 and positive but not significant for the *C. edule* & *M. balthica* and *S. plana* & *H. diversicolor* duos. This  
 318 could suggest that the two duos of species contribute equally to the formation of the fluff layer. The  
 319 slopes for the duo *C. volutator* & *P. ulvae* have confidence intervals that are too wide to be considered  
 320 conclusive (details in Supplementary data 3.2.2 SuppFig 3.K SuppTab 3.I)



321

322 *Figure 6 Fluff layer quantity ( $Q_{fluff}$  [ $g \cdot m^{-2}$ ]) vs the different metabolic rate evaluation [ $mW \cdot m^{-2}$ ]: based*  
 323 *on the measured respiration rate  $Itot_{respi}$  (A), the  $Itot$  with the mesocosm temperature  $Itot_{meso}$  (B) and the*  
 324  *$Itot$  with the flume temperature  $Itot_{flume}$  (C) and their regression line. Note that the y scale is Box-Cox*  
 325 *transformed, and the models were made on transformed data.*



326 *Figure 7 Right column: results for transformed  $Q_{fluff}$  - A1) ANCOVA model using the temperature as*  
 327 *factor and the  $Itot_{meso}$  as covariant; A2) ANCOVA model using the duos as factor and the  $Itot_{meso}$  as*  
 328 *covariant; Left column: results for transformed  $BSS_{mass}$  - B1) ANCOVA model using the temperature as*

329 factor and the  $Itot_{meso}$  as covariant; B2) ANCOVA model using the duos as factor and the  $Itot_{meso}$  as  
 330 covariant. Filled dot are  $p$ -value  $\leq 0.1$  and empty dot are  $p$ -value  $> 0.1$ .

331

332 Table 1 Linear regression estimates for each species  $Itot_{meso}$  ( $y = Intercept + \beta_{S1} \cdot S1 + \beta_{S2} \cdot S2$ ), with  
 333 95% confidence interval in all experiments and by duos separated for  $Q_{fluff}$  and  $BSS_{mass}$ .

	Intercept	$\beta_{S1}$	$\beta_{S2}$	R <sup>2</sup>	N
<b>Fluff layer : <math>Q_{fluff}</math></b>					
All	9.24e <sup>-01</sup> [9.23e <sup>-01</sup> , 9.25e <sup>-01</sup> ]	2.67e <sup>-05</sup> [6.85e <sup>-06</sup> , 4.65e <sup>-05</sup> ]	2.94e <sup>-05</sup> [1.29e <sup>-05</sup> , 4.59e <sup>-05</sup> ]	0.177***	86
C. edule & M. balthica	9.25e <sup>-01</sup> [9.21e <sup>-01</sup> , 9.30e <sup>-01</sup> ]	8.53e <sup>-06</sup> [-3.92e <sup>-05</sup> , 5.62e <sup>-05</sup> ]	2.43e <sup>-05</sup> [-1.36e <sup>-05</sup> , 6.23e <sup>-05</sup> ]	0.089	25
Control	9.24e <sup>-01</sup> [9.22e <sup>-01</sup> , 9.25e <sup>-01</sup> ]	-	-	-	14
C. volutator & P. ulvae	9.23e <sup>-01</sup> [9.20e <sup>-01</sup> , 9.27e <sup>-01</sup> ]	3.44e <sup>-04</sup> [-2.04e <sup>-04</sup> , 8.92e <sup>-04</sup> ]	-9.87e <sup>-06</sup> [-4.10e <sup>-04</sup> , 3.90e <sup>-04</sup> ]	0.168	24
S. plana & H. diversicolor	9.24e <sup>-01</sup> [9.21e <sup>-01</sup> , 9.27e <sup>-01</sup> ]	4.03e <sup>-05</sup> [-1.38e <sup>-05</sup> , 9.44e <sup>-05</sup> ]	4.98e <sup>-06</sup> [-6.03e <sup>-05</sup> , 7.03e <sup>-05</sup> ]	0.144	23
<b>Mass erosion threshold : <math>BSS_{mass}</math></b>					
All	6.73e <sup>-01</sup> [6.32e <sup>-01</sup> , 7.14e <sup>-01</sup> ]	-1.87e <sup>-03</sup> [-2.74e <sup>-03</sup> , -1.01e <sup>-03</sup> ]	-1.33e <sup>-03</sup> [-2.05e <sup>-03</sup> , -6.08e <sup>-04</sup> ]	0.262****	84
C. edule & M. balthica	4.56e <sup>-01</sup> [3.08e <sup>-01</sup> , 6.04e <sup>-01</sup> ]	4.78e <sup>-04</sup> [-1.11e <sup>-03</sup> , 2.07e <sup>-03</sup> ]	7.63e <sup>-05</sup> [-1.19e <sup>-03</sup> , 1.34e <sup>-03</sup> ]	0.023	25
Control	6.52e <sup>-01</sup> [5.87e <sup>-01</sup> , 7.17e <sup>-01</sup> ]	-	-	-	13
C. volutator & P. ulvae	4.93e <sup>-01</sup> [3.54e <sup>-01</sup> , 6.33e <sup>-01</sup> ]	3.37e <sup>-02</sup> [1.33e <sup>-02</sup> , 5.41e <sup>-02</sup> ]	2.75e <sup>-02</sup> [1.25e <sup>-02</sup> , 4.25e <sup>-02</sup> ]	0.434**	23
S. plana & H. diversicolor	5.73e <sup>-01</sup> [4.67e <sup>-01</sup> , 6.80e <sup>-01</sup> ]	-1.69e <sup>-03</sup> [-3.59e <sup>-03</sup> , 2.06e <sup>-04</sup> ]	7.32e <sup>-04</sup> [-1.56e <sup>-03</sup> , 3.02e <sup>-03</sup> ]	0.299*	23

334

### 335 3.2.3 Mass erosion

336 The threshold for mass erosion bed shear stress ( $BSS_{mass}$  [Pa]) showed a high dispersion in regard  
 337 of any of the three different ways to evaluate the metabolic rate of the sample (Figure 8).  $BSS_{mass}$  was  
 338 measured for controls at 1.40 $\pm$ 0.51 Pa (n = 14), *C. edule* & *M. balthica* at 0.84 $\pm$ 0.36 Pa (n = 25), *S.*  
 339 *plana* & *H. diversicolor* at 1.00 $\pm$ 0.34 Pa (n = 23) and *C. volutator* & *P. ulvae* at 1.88 $\pm$ 0.73 Pa (n = 24)

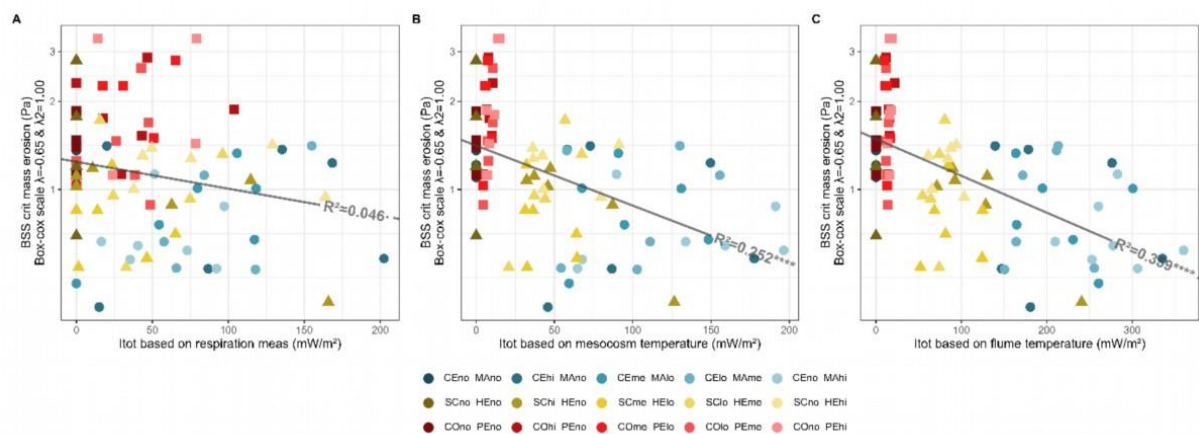
340 A linear model of  $BSS_{mass}$  versus  $Itot$  showed a low value of indicator R<sup>2</sup>, the  $Itot_{flume}$  being with the  
 341 best (R<sup>2</sup> = 0.339\*\*\*\*), followed by  $Itot_{meso}$  (R<sup>2</sup> = 0.252\*\*\*\*),  $Itot_{respi}$  (R<sup>2</sup> = 0.046) being the lowest (Figure  
 342 8). An ANCOVA was conducted on  $BSS_{mass}$  transformed as dependent variable, with  $Itot_{meso}$  as covariant  
 343 and temperature as factor (F<sub>(2,80)</sub> = 7.76, p = 0.0008, Figure 7-B1, details in Supplementary data 3.2.3  
 344 SuppTab 3.K, N). There was a significant effect of the metabolic rate but also a significant effect of the  
 345 temperatures (p<0.1). In detail, the low temperature had significant negative effect on the  $BSS_{mass}$ , when  
 346 high temperature has a significant positive effect (a negative effect lowers the erosion threshold and  
 347 therefore increases erodibility). These results showed that the temperature has supplementary effect  
 348 than the one from the metabolic activity of the fauna.

349 An ANCOVA was conducted on  $BSS_{mass}$  transformed as dependent variable, with  $Itot_{meso}$  as  
 350 covariant and duos as factor (F<sub>(3,79)</sub> = 8.39, p<0.0001, Figure 7-B2, details in Supplementary data 3.2.3



351 SuppTab 3.L, N). There was no significant effect of the metabolic rate but significant differences between  
 352 three duos ( $p < 0.1$ ). In detail, the duos *C. edule* & *M. balthica* and *S. plana* & *H. diversicolor* had  
 353 significant negative effects not significantly different on the  $BSS_{mass}$ , when the *C. volutator* & *P. ulvae*  
 354 have a significant positive effect compared to the controls. These results showed that independently of  
 355 the metabolic rate in the range of this experiment, the duo *C. edule* & *M. balthica* would destabilize the  
 356 sediment more than *S. plana* & *H. diversicolor*, and that *C. volutator* & *P. ulvae* could have a stabilizing  
 357 effect compared to an abiotic sediment.

358 The linear regressions of  $BSS_{mass}$  as a function of the two metabolic rates of each species within the  
 359 duos had a  $R^2$  similar to that of the  $Itot_{meso}$  as a whole ( $R^2 = 0.262^{****}$ ,  $n = 84$ , Table 1). The slopes of  
 360 the two species are significantly similar and negative for all duos. However, the duo *C. edule* & *M.*  
 361 *balthica* showed almost no effect for both species, without significance, and *S. plana* & *H. diversicolor*  
 362 showed a slightly asymmetric effect, slightly positive for *H. diversicolor* and negative for *S. plana*, but  
 363 without significance. Slopes for *C. volutator* & *P. ulvae* are significantly positive, slightly higher for *C.*  
 364 *volutator*, but with very wide confidence intervals (details in Supplementary data 3.2.2 SuppFig 3.R  
 365 SuppTab 3.O).



366

367 *Figure 8 Critical bed shear stress ( $BSS_{mass}$  [Pa] vs the different metabolic rate evaluation [ $mW \cdot m^{-2}$ ]:*  
 368 *the measured respiration rate  $Itot_{respi}$  (A), the  $Itot$  with the mesocosm temperature  $Itot_{meso}$  (B) and the  $Itot$*   
 369 *with the flume temperature  $Itot_{flume}$  (C) and their regression line. Note that the scales are Box-Cox*  
 370 *transformed, and the models were made on transformed data.*

## 371 4 Discussion

### 372 4.1 Metabolic rate and physiologic state of individuals

373 By measuring the respiratory rate of the animals in each sample, we sought to verify the relevance  
 374 of the basal metabolic rate model and achieve the first objective of the study. However, the results  
 375 showed a high variability, which can be attributed primarily to the experimental conditions that could  
 376 affect the physiological state of animals or their behaviour.

377 Firstly, small mobile fauna such as *C. volutator* and *H. diversicolor* were unable to bury themselves  
378 during the respiration measurement (only water in the chamber). They were therefore forced to swim  
379 actively in the stirred water, which is not entirely representative of a natural activity. For comparison, the  
380 respiration rate of *H. diversicolor* showed results 10 to 25 times higher than obtained by Galasso  
381 (Galasso et al., 2018) (see Supplementary data 2.1 SuppTab 2.B). This may explain the differences  
382 observed in the slopes by duos in Figure 4, as the measurement conditions were relatively optimal for  
383 molluscs but lead to a higher respiration level for the others due to the stress induced by the  
384 measurement.

385 Secondly, the ANCOVA showing a significant difference for medium (spring) temperature is also the  
386 result of the experimental conditions. Measurements at this temperature were carried out at the  
387 beginning of experiments using animals recently taken from the natural environment and placed in a  
388 mesocosm at a temperature very close to the temperature of the environment at the time of sampling  
389 (see Supplementary data 2.4 SuppFig 2.L). The individuals were therefore in a state of minimal stress  
390 and in a physiological state as close as possible to their natural state. As the experiment progressed,  
391 the fauna was collected over a period of two months, with some individuals being kept in the mesocosm  
392 for the duration of the experiment and others being sampled shortly before the experiment. Noticeably,  
393 this period was marked by a heat wave - which was reflected in the temperature of the flume water -  
394 and may have had an effect on the physiological state of the animals that were taken last. Furthermore,  
395 no tests were carried out on the animals after the erosion had been measured, to assess possible  
396 parasitism or the state of their energy reserves, for example. This was partly due to a technical  
397 impossibility, as many of the animals were swept away by the current and destroyed by the circulation  
398 in the pump.

399 All those experimental biases explain the variability in respiration measurements, and explain the  
400 performance of the correlation with the basal metabolic rate model. But overall, the metabolic rate model  
401 is sufficiently valid for all species combined. The  $Itot$  parameterization is broad in its classification,  
402 separating the invertebrate phylogenetic tree into "only" 19 categories, here *C. edule*, *M. balthica* and  
403 *S. plana* were calculated with the same parameters. This is a good point for generalization and  
404 simplification that could be useful from a modelling point of view.

## 405 4.2 Temperature effect on bioturbation activity

406 The second objective of this study was to assess the effect of temperature variation on metabolism  
407 and its consequence on bioturbation and sediment erodibility. Respiration measurements showed that  
408 the animals used throughout the experiment were not in the same physiological state, hence the interest  
409 in comparing erodibility results with  $Itot_{respi}$  and  $Itot_{meso}$ . It should be noted that the temperature in the  
410 protocol affects not only the animals but also the sediment. A positive correlation was observed between  
411 temperature and sediment erodibility (decrease in BSS erosion threshold, increase in erosion flux),  
412 although empirical studies have not ruled out the nature of the relationship between the two variables

413 (Grabowski et al., 2011). In an ANOVA using controls alone according to temperature, there was no  
414 significant difference for any of the erodimetry parameters between the 3 temperature levels, but a shift  
415 was observed reflecting a facilitation of erosion with increasing temperature, more pronounced for the  
416 summer temperature (see Supplementary data 3.2.1 SuppFig 3.E).

417 There were three methods of calculating the metabolic rate, which we have chosen to present,  
418 although the metabolic rate based on mesocosm temperature ( $Itot_{meso}$ ) remains our reference. The use  
419 of respiration data ( $Itot_{respi}$ ) added a significant degree of uncertainty and variability, the origin of which  
420 is mostly experimental. As the erodimetry results are also subject to biases that create variability, we  
421 chose not to use the respirometry results as a reference for the statistical tests, but only to validate that  
422 the metabolic rate model was relevant, as it is a tool for functional modelling of the environment.

423 On the other hand, displaying the results with the metabolic rate calculated with the temperature in  
424 the flume ( $Itot_{flume}$ ) serves several purposes. Firstly, this result highlights the need to design experimental  
425 protocols that do not introduce biases of this magnitude. Indeed, we should have worked in erodimetry  
426 with water at a temperature similar to the mesocosm, or best in a climatic room, but technical limitations  
427 prevented us from doing so. The better performance of the model with flume temperature is probably a  
428 mathematical artefact, as the range of  $Itot_{flume}$  values is wider than with  $Itot_{meso}$ , without the erosion  
429 parameter being modified.

430 However, the difference in temperature between the mesocosm and the flume raises the question of  
431 the speed of thermal adaptation of these species, which originate from the intertidal zone and thus  
432 experience considerable variations in environmental conditions over the course of a day. Settling in the  
433 sediment can buffer the variations in temperature, but feeding, particularly by filtering, puts the individual  
434 in close and immediate contact with water whose temperature can vary. If we were to consider the rapid  
435 change in temperature as a thermal shock, then Brey's model would no longer be appropriate, because  
436 it models a static metabolism, not a dynamic one. In general, metabolic models are defined under long-  
437 term stable temperature conditions, but are unable to reproduce thermal stress. On the other hand, we  
438 could consider that this type of variation is of the order of magnitude that these organisms experience  
439 daily. What are the kinetics of adaptation of the different species to these dynamic variations remains to  
440 be clarified.

441 Moreover, being a linear relationship limited by bounds, metabolic models exclude any possibility of  
442 extrapolation outside the observed range. Recent *in situ* observations have shown that the activity and  
443 therefore the magnitude of the bioturbation effects can vary according to the season, with a range of low  
444 temperatures well below those examined in this study (Morelle et al., 2024). In winter, *H. diversicolor*  
445 appears to maintain its stabilizing effect, while *S. plana* no longer has a significant effect. It was  
446 hypothesized that the abiotic winter conditions have a greater effect on sediment transport than the  
447 biological effect due to reduced biological activity in winter.

448 Finally, there is the question of what bioturbation is being measured. The experimental protocol of  
449 this study was designed to measure mainly the result of the integration of a period of bioturbation, rather  
450 than the immediate bioturbation that may occur during the measurement. This is due to the time  
451 difference between these two phases (more than 6h of bioturbation, and less than 2h for erodimetry),  
452 particularly regarding the fluff layer. The mechanisms of chronic bioturbation are linked to the living and  
453 feeding environment as well as the tidal cycle. A grazing epibenthic species will produce surface traces  
454 associated with its crawling time at low tide (Orvain and Sauriau, 2002), whereas a suspension-feeding  
455 endobenthic species will produce an immediate and continuous biogenic layer at high tide. We can see  
456 the role that the dynamics of metabolic adaptation could also play in the effects of bioturbation on bed  
457 erodibility, for example with “fight or flight” strategies such as sinking into sediments in inhospitable  
458 conditions, as Zhou showed in the case of a heat wave (Zhou, 2023).

## 459 4.3 Effects of species combination bioturbation on sediment erodibility

### 460 4.3.1 Fluff layer resuspension

461 The erosion of the fluff layer appears to be explained by the metabolic rate of the fauna present in  
462 the sediment, whatever the species. However, this result must be qualified by the discrepancy of the  
463 results. This is because  $Q_{fluff}$  determination is an indirect method that inherently involves a high degree  
464 of uncertainty. It depends on the height and duration of the erosion measurement steps, with threshold  
465 effects which, depending on the decision to attribute a step to fluff or mass, can significantly vary the  
466  $Q_{fluff}$  value (Dairain et al., 2020b). In addition, the fluff layer is created in the incubation core, which is  
467 transferred to the sample bearer for erosion measurement, producing disturbances on the sample that  
468 were minimized as much as possible, but could not be totally avoided.

469 The  $Q_{fluff}$  was normalised by a Box-Cox transformation with a  $\lambda$  close to -1, *i.e.* an inverse  
470 transformation. The linear regression of the transformed data then corresponds to a linear relationship  
471 for the raw data. The choice of defining a simple linear relationship was intended to highlight the  
472 relationship between the two parameters, without over-interpreting it given the variability of the results.  
473 The relation between  $Itot_{meso}$  and  $Q_{fluff}$  is probably more modelled by an asymptotic von Bertalanffy  
474 relationship, as could have been observed for *C. edule* (Lehuen and Orvain, 2024), and used in other  
475 studies like for *P. ulvae* (Orvain and Sauriau, 2002), for *S. plana* (Orvain, 2005), or *M. balthica* (Willows  
476 et al., 1998).

477 The results of the study of (Cozzoli et al., 2018), with *C. edule*, *M. balthica*, *S. plana*, *H. diversicolor*  
478 and *C. volutator* isolated, showed some similar scales of results for  $Q_{fluff}$  but with a quicker dynamic  
479 (critical fluff BSS lower) and global asymptotical with a clearer trend (details in Supplementary data 3.2.1  
480 SuppFig 3.F). This trend difference may be mainly due to the fact that there were made on different  
481 flumes and with a different way to prepare the sediment, as shown by the records of controls, and as  
482 seen in a meta-analysis of erodibility studies (Lehuen and Orvain, 2024).

483 Overall, the presence of metabolic energy explains the creation of an easily erodible sedimentary  
484 layer, which can be attributed to the bioturbation action of the fauna present. Although the results are  
485 very noisy, they suggest that metabolic rate is an interesting way of describing surface bioturbation  
486 phenomena and a generic model could be sought, which could facilitate the integration of these  
487 processes in sediment transport models.

#### 488 4.3.2 Mass erosion

489 Bioturbation can modify the constitutive layer of sediments, facilitating or hindering mass erosion at  
490 high bed shear stress: *S. plana* was observed as a deep destabilizing species, reducing the critical  
491 threshold of mass erosion (Orvain, 2005); on the other hand, a stabilizing effect was attributed to the  
492 worm *H. diversicolor* (Passarelli et al., 2014). The processes involved take place in subsurface sediment  
493 and are closely linked to the history of settlement of the individual in the sediment.

494 The results of this study tend to indicate that the metabolic rate is not a suitable descriptor for  
495 assessing the effects of bioturbation on sediment mass erodibility. Despite very noisy results, the  
496 ANCOVA did not show a statistical link between metabolic rate and mass erosion threshold, but did  
497 show significant differences depending on the species duos. On the one hand, *C. edule* & *M. balthica*  
498 and *S. plana* & *H. diversicolor* would have a destabilising effect, more marked for *C. edule* & *M. balthica*,  
499 on the other hand, *C. volutator* & *P. ulvae* duo appears to have a stabilizing effect.

500 In the case of *S. plana* & *H. diversicolor*, it appears that the destabilising effect of *S. plana* is more  
501 pronounced than the stabilising effect of *H. diversicolor* in the experiment temperature range. Although  
502 the results seem to indicate that *S. plana* and *H. diversicolor* have antagonistic effects on sediment  
503 erodibility, the number of experiments performed did not allow us to distinguish them significantly.  
504 (Morelle et al., 2024) observed *in situ* at summer conditions this antagonistic effects of the two species.  
505 However, this study does not provide any information on the hydrodynamic conditions during the  
506 measured bioturbation period. It is likely that these conditions were of the order of chronic effects rather  
507 than the strong hydrodynamic conditions associated with mass erosion. As de Smit observed (de Smit  
508 et al., 2021a, 2021b), the behaviour of *H. diversicolor* could be modified by the presence of other species  
509 in the sample, preventing the stabilization effect from being significantly expressed. This interacting  
510 mechanism should be described with further details.

511 As far as the *C. edule* & *M. balthica* duo is concerned, the effect of mass destabilisation is generally  
512 little or no highlighted in the literature for these two species (see Supplementary data 2.1 SuppFig 2.C  
513 SuppTab 2.C). An analogy could be made between *M. balthica* and *S. plana* and therefore on its effects,  
514 for a smaller species but installed less deeply. However, in the case of *C. edule*, its impact on erodibility  
515 relates more to the surface, and is generally linked to its movements and the generation of intrinsic  
516 roughness (Dairain et al., 2020b). In our experimental conditions, the presence of *C. edule*, and to a  
517 lesser extent *M. balthica*, generated fragilities on the sediment surface during transfers from the cores  
518 to the sample bearer in the flume, which may have facilitated mass erosion. These fragilities also

519 exposed the individuals to the currents, causing *C. edule* to sink into the sediment during phases of  
520 strong currents, facilitating mass erosion.

521 Finally, for *C. volutator* & *P. ulvae*, these two species live on the surface of sediment. *P. ulvae* was  
522 already identified as a bioturbator not able to change the mass erosion critical threshold (Orvain, 2005;  
523 Orvain et al., 2003). In addition, there were no observation of effect of *C. volutator* on mass erosion by  
524 (Grant and Daborn, 1994). It is important to note that the experimental methodology for *C. volutator* &  
525 *P. ulvae* was different to the others duos. Their bioturbation period was made in the absence of high  
526 tide, it was not possible for *C. volutator* to dig a gallery, which it did in the flume as soon as it was put in  
527 the water, as observed in (De Backer et al., 2010). In addition, the bioturbation phase took place in the  
528 sample bearer and not in the incubation core, thus eliminating a disturbance phase present in all the  
529 measurements of the other two duos. This was a limitation of this protocol which, due to the design of  
530 the flume, did not allow equivalent treatment for surface and sub-surface species.

#### 531 4.4 Toward a community erosion model

532 This study illustrates the potential importance of missing data when modelling the bioturbation effects  
533 on sediment erodibility. However, due to several biases and experimental limitations, the data set was  
534 noisy enough to prevent modelling of the bioturbation effect of combined species on erodibility that could  
535 be incorporated into HMS models.

536 Nevertheless, our results suggest that this route is sufficiently relevant for the fluff layer erosion to  
537 be pursued with this type of experiment, with fewer factors and more controlled conditions to guarantee  
538 a higher degree of accuracy. An assessment of the impact of temperature on the effects of bioturbation  
539 on sediment erodibility for isolated species, taking into account the kinetics of metabolic adaptation is  
540 clearly required. According to (Kooijman, 2010), metabolic adaptation to a new temperature is rather  
541 slow (days to weeks). However, intertidal animals are subject to very wide temperature conditions, so  
542 they should have a range of metabolic functions that allow them to adapt. In any case, the *Itot* calculation  
543 is only applicable in the range of temperatures valid for the organism.

544 The metabolic rate is a good descriptor to link the fauna activity to the chronic bioturbation effect, but  
545 is not adequate to combine several species as a community considering mass erosion (event-driven  
546 effects), regardless of their type of bioturbation activity. A simple categorisation were made by depth of  
547 living for fauna in (Cozzoli et al., 2018) for example. Indeed, the variety of bioturbation processes and  
548 their impact on sediment erodibility shows that the question of metabolic energy alone may be  
549 insufficient, and may explain the level of dispersion of the results obtained in the present study.  
550 Moreover, the experimental conditions in the bibliography used to classify these species were very  
551 diversified, depending on the sediment types, the measurement methods, or the mesocosm conditions  
552 (presence/absence of microphytobenthic biofilm for instance) and bioturbation behaviours and  
553 acclimation.

554 Among the many methodological differences in all the existing studies, one aspect seems key: the  
555 presence or absence of MPB biofilm on the sediment surface. Deposit feeder species have often been  
556 classified as destabilizing, either chronically or event-driven, because they graze biofilm, which has a  
557 strong stabilising effect (Andersen et al., 2002; de Deckere et al., 2000; Orvain et al., 2014a, 2004; van  
558 Prooijen et al., 2011). The effects measured in laboratory experiments without MPB do not take into  
559 account a key element of *in situ* conditions. In the environment, the properties of the sediment on the  
560 surface are the result of a synergy between the bioturbating fauna and the MPB, with the former altering  
561 the effects of the latter. There is therefore often a discrepancy between laboratory and *in situ* results, to  
562 say it roughly: in the laboratory we measure the characteristics of the sediment itself (unless intended  
563 inoculation), in the field the characteristics of the MPB biofilm (Andersen et al., 2010, 2005; Orvain et  
564 al., 2004).

## 565 5 Conclusion

566 This study aimed at revealing how macrozoobenthic communities and temperature could modify the  
567 sediment erodibility parameters. By coupling two species, we showed that the metabolic rate was an  
568 interesting descriptor for modelling sediment transport at the community scale for the creation of fluff  
569 layer. The effects of bioturbation on mass erosion appeared to require another information rather the  
570 metabolic rate, information that the bioturbation functional group could provide, even if the destabilizing  
571 effects on the constitutive layer of sediment seemed to dominate, at least in the absence of MPB. The  
572 kinetics of metabolic acclimatisation still need to be explored to determine how reactive the individual  
573 might be, in order to settle the question of how metabolic rate is taken into account in a model. The  
574 effect of fauna and their bioturbation activity regarding the temperature condition through the metabolic  
575 rate is a prerequisite to model at large spatial and temporal scales the impact of fauna on their habitat,  
576 and especially to integrate this process into hydro-morpho-sedimentary models of ecosystems such as  
577 estuaries.

578

### 579 ACKNOWLEDGEMENT

580 The authors thank Maxime Cottin for his help on the field and with the flume experiments. The authors  
581 acknowledge anonymous reviewers for their valuable comments and suggestions.

### 582 FUNDING

583 This research was supported by the *Région Normandie* for the A. Lehuen PhD and funded by the  
584 *Office Français pour la Biodiversité* for the MELTING POTES project.

### 585 CREDIT AUTHOR STATEMENT

586 A. Lehuen: Conceptualization, Methodology, Formal analysis, Data Curation, Writing - Original Draft,  
587 Funding acquisition ; R. Oulhen: Methodology, Data Curation ; Z. Zhou: Conceptualization,

588 Methodology, Writing - Review & Editing ; J. de Smit: Conceptualization, Methodology, Writing - Review  
589 & Editing ; L. van Ijzerloo: Methodology ; F. Cozzoli: Conceptualization, Methodology, Writing - Review  
590 & Editing ; T. Bouma: Conceptualization, Resources, Supervision ; F. Orvain: Conceptualization,  
591 Methodology, Formal analysis, Resources, Writing - Review & Editing, Supervision, Project  
592 administration, Funding acquisition

## 593 **References**

- 594 Allen, A.P., Gillooly, J.F., Brown, J.H., 2005. Linking the global carbon cycle to individual metabolism.  
595 *Funct. Ecol.* 19, 202–213. <https://doi.org/10.1111/j.1365-2435.2005.00952.x>
- 596 Andersen, T.J., Jensen, K.T., Lund-Hansen, L., Mouritsen, K.N., Pejrup, M., 2002. Enhanced erodibility  
597 of fine-grained marine sediments by *Hydrobia ulvae*. *J. Sea Res.* 48, 51–58.  
598 [https://doi.org/10.1016/S1385-1101\(02\)00130-2](https://doi.org/10.1016/S1385-1101(02)00130-2)
- 599 Andersen, T.J., Lanuru, M., Van Bernem, C., Pejrup, M., Riethmueller, R., 2010. Erodibility of a mixed  
600 mudflat dominated by microphytobenthos and *Cerastoderma edule*, East Frisian Wadden Sea,  
601 Germany. *Estuar. Coast. Shelf Sci.*, Mechanisms of sediment retention in estuaries 87, 197–  
602 206. <https://doi.org/10.1016/j.ecss.2009.10.014>
- 603 Andersen, T.J., Lund-Hansen, L.C., Pejrup, M., Jensen, K.T., Mouritsen, K.N., 2005. Biologically  
604 induced differences in erodibility and aggregation of subtidal and intertidal sediments: a possible  
605 cause for seasonal changes in sediment deposition. *J. Mar. Syst.* 55, 123–138.  
606 <https://doi.org/10.1016/j.jmarsys.2004.09.004>
- 607 Bocher, P., Piersma, T., Dekinga, A., Kraan, C., Yates, M.G., Guyot, T., Folmer, E.O., Radenac, G.,  
608 2007. Site- and species-specific distribution patterns of molluscs at five intertidal soft-sediment  
609 areas in northwest Europe during a single winter. *Mar. Biol.* 151, 577–594.  
610 <https://doi.org/10.1007/s00227-006-0500-4>
- 611 Brey, T., 2010. An empirical model for estimating aquatic invertebrate respiration: Aquatic invertebrate  
612 respiration. *Methods Ecol. Evol.* 1, 92–101. <https://doi.org/10.1111/j.2041-210X.2009.00008.x>
- 613 Brey, T., Müller-Wiegmann, C., Zittier, Z.M.C., Hagen, W., 2010. Body composition in aquatic organisms  
614 — A global data bank of relationships between mass, elemental composition and energy  
615 content. *J. Sea Res.* 64, 334–340. <https://doi.org/10.1016/j.seares.2010.05.002>
- 616 Brown, J.H., Gillooly, J.F., Allen, A.P., Savage, V.M., West, G.B., 2004. Toward a metabolic theory of  
617 ecology. *Ecology* 85, 1771–1789. <https://doi.org/10.1890/03-9000>
- 618 Brückner, M.Z.M., Schwarz, C., Coco, G., Baar, A., Boechat Albernaz, M., Kleinhans, M.G., 2021.  
619 Benthic species as mud patrol - modelled effects of bioturbators and biofilms on large-scale  
620 estuarine mud and morphology. *Earth Surf. Process. Landf.* 46, 1128–1144.  
621 <https://doi.org/10.1002/esp.5080>
- 622 Carleton Ray, G., McCormick-Ray, J., 2013. Estuarine Ecosystems, in: *Encyclopedia of Biodiversity*.  
623 Elsevier, pp. 297–308. <https://doi.org/10.1016/B978-0-12-384719-5.00244-6>
- 624 Cozzoli, F., Bouma, T.J., Ottolander, P., Lluch, M.S., Ysebaert, T., Herman, P.M.J., 2018. The combined  
625 influence of body size and density on cohesive sediment resuspension by bioturbators. *Sci.*  
626 *Rep.* 8, 3831. <https://doi.org/10.1038/s41598-018-22190-3>
- 627 Cozzoli, F., Gjoni, V., Del Pasqua, M., Hu, Z., Ysebaert, T., Herman, P.M.J., Bouma, T.J., 2019. A  
628 process based model of cohesive sediment resuspension under bioturbators' influence. *Sci.*  
629 *Total Environ.* 670, 18–30. <https://doi.org/10.1016/j.scitotenv.2019.03.085>
- 630 Cozzoli, F., Shokri, M., da Conceição, T.G., Herman, P.M.J., Hu, Z., Soissons, L.M., Van Dalen, J.,  
631 Ysebaert, T., Bouma, T.J., 2021. Modelling spatial and temporal patterns in bioturbator effects  
632 on sediment resuspension: A biophysical metabolic approach. *Sci. Total Environ.* 148215.  
633 <https://doi.org/10.1016/j.scitotenv.2021.148215>
- 634 Dairain, A., Maire, O., Meynard, G., Orvain, F., 2020a. Does parasitism influence sediment stability?  
635 Evaluation of trait-mediated effects of the trematode *Bucephalus minimus* on the key role of



636           cockles *Cerastoderma edule* in sediment erosion dynamics. *Sci. Total Environ.* 733, 139307.  
637           <https://doi.org/10.1016/j.scitotenv.2020.139307>

638   Dairain, A., Maire, O., Meynard, G., Richard, A., Rodolfo-Damiano, T., Orvain, F., 2020b. Sediment  
639   stability: can we disentangle the effect of bioturbating species on sediment erodibility from their  
640   impact on sediment roughness? *Mar. Environ. Res.* 162, 105147.  
641   <https://doi.org/10.1016/j.marenvres.2020.105147>

642   De Backer, A., Van Ael, E., Vincx, M., Degraer, S., 2010. Behaviour and time allocation of the mud  
643   shrimp, *Corophium volutator*, during the tidal cycle: a laboratory study. *Helgol. Mar. Res.* 64,  
644   63–67. <https://doi.org/10.1007/s10152-009-0167-6>

645   de Deckere, E.M.G.T., Tolhurst, T.J., de Brouwer, J.F.C., 2001. Destabilization of Cohesive Intertidal  
646   Sediments by Infauna. *Estuar. Coast. Shelf Sci.* 53, 665–669.  
647   <https://doi.org/10.1006/ecss.2001.0811>

648   de Deckere, E.M.G.T., van de Koppel, J., Heip, C.H.R., 2000. The influence of *Corophium volutator*  
649   abundance on resuspension. *Hydrobiologia* 426, 37–42.  
650   <https://doi.org/10.1023/A:1003978714382>

651   de Smit, J.C., Brückner, M.Z.M., Mesdag, K.I., Kleinhans, M.G., Bouma, T.J., 2021a. Key Bioturbator  
652   Species Within Benthic Communities Determine Sediment Resuspension Thresholds. *Front.*  
653   *Mar. Sci.* 8, 1344. <https://doi.org/10.3389/fmars.2021.726238>

654   de Smit, J.C., Kleinhans, M.G., Gerkema, T., Bouma, T.J., 2021b. Quantifying natural sediment  
655   erodibility using a mobile oscillatory flow channel. *Estuar. Coast. Shelf Sci.* 262, 107574.  
656   <https://doi.org/10.1016/j.ecss.2021.107574>

657   Ettema, C.H., Wardle, D.A., 2002. Spatial soil ecology. *Trends Ecol. Evol.* 17, 177–183.  
658   [https://doi.org/10.1016/S0169-5347\(02\)02496-5](https://doi.org/10.1016/S0169-5347(02)02496-5)

659   European Environment Agency, 2023. EUNIS -EUNIS habitat types hierarchical view - revised groups  
660   [WWW Document]. URL <https://eunis.eea.europa.eu/habitats-code-browser-revised.jsp>  
661   (accessed 8.2.23).

662   Galasso, H., Richard, M., Lefebvre, S., Aliaume, C., Callier, M., 2018. Body size and temperature effects  
663   on standard metabolic rate for determining metabolic scope for activity of the polychaete *Hediste*  
664   (*Nereis*) *diversicolor*. *PeerJ* 6, e5675. <https://doi.org/10.7717/peerj.5675>

665   Glazier, D.S., 2022. Variable metabolic scaling breaks the law: from ‘Newtonian’ to ‘Darwinian’  
666   approaches. *Proc. R. Soc. B Biol. Sci.* 289, 20221605. <https://doi.org/10.1098/rspb.2022.1605>

667   Grabowski, R.C., Droppo, I.G., Wharton, G., 2011. Erodibility of cohesive sediment: The importance of  
668   sediment properties. *Earth-Sci. Rev.* 105, 101–120.  
669   <https://doi.org/10.1016/j.earscirev.2011.01.008>

670   Grant, J., Daborn, G., 1994. The effects of bioturbation on sediment transport on an intertidal mudflat.  
671   *Neth. J. Sea Res.* 32, 63–72. [https://doi.org/10.1016/0077-7579\(94\)90028-0](https://doi.org/10.1016/0077-7579(94)90028-0)

672   Guizien, K., Orvain, F., Duchêne, J.-C., Le Hir, P., 2012. Accounting for Rough Bed Friction Factors of  
673   Mud Beds as a Result of Biological Activity in Erosion Experiments. *J. Hydraul. Eng.* 138, 979–  
674   984. [https://doi.org/10.1061/\(ASCE\)HY.1943-7900.0000627](https://doi.org/10.1061/(ASCE)HY.1943-7900.0000627)

675   Hewitt, J.E., Thrush, S.F., Halliday, J., Duffy, C., 2005. The Importance of Small-Scale Habitat Structure  
676   for Maintaining Beta Diversity. *Ecology* 86, 1619–1626. <https://doi.org/10.1890/04-1099>

677   Huey, R.B., Kingsolver, J.G., 2019. Climate Warming, Resource Availability, and the Metabolic  
678   Meltdown of Ectotherms. *Am. Nat.* 194, E140–E150. <https://doi.org/10.1086/705679>

679   Jones, C.G., Lawton, J.H., Shachak, M., 1997. Positive and Negative Effects of Organisms as Physical  
680   Ecosystem Engineers. *Ecology* 78, 1946–1957. [https://doi.org/10.1890/0012-9658\(1997\)078\[1946:PANEOO\]2.0.CO;2](https://doi.org/10.1890/0012-9658(1997)078[1946:PANEOO]2.0.CO;2)

682   Jones, C.G., Lawton, J.H., Shachak, M., 1994. Organisms as Ecosystem Engineers. *Oikos* 69, 373–  
683   386. <https://doi.org/10.2307/3545850>

684   Kassambara, A., 2023. rstatix: Pipe-Friendly Framework for Basic Statistical Tests • rstatix [WWW  
685   Document]. URL <https://rpkgs.datanovia.com/rstatix/> (accessed 2.26.24).

- 686 Kooijman, S.A.L.M., 2010. *Dynamic Energy Budget Theory for Metabolic Organisation*. Cambridge  
687 University Press.
- 688 Kristensen, E., Neto, J.M., Lundkvist, M., Frederiksen, L., Pardal, M.Â., Valdemarsen, T., Flindt, M.R.,  
689 2013. Influence of benthic macroinvertebrates on the erodability of estuarine cohesive  
690 sediments: Density- and biomass-specific responses. *Estuar. Coast. Shelf Sci.* 134, 80–87.  
691 <https://doi.org/10.1016/j.ecss.2013.09.020>
- 692 Kristensen, E., Penha-Lopes, G., Delefosse, M., Valdemarsen, T., Quintana, C.O., Banta, G.T., 2012.  
693 What is bioturbation? The need for a precise definition for fauna in aquatic sciences. *Mar. Ecol.*  
694 *Prog. Ser.* 446, 285–302. <https://doi.org/10.3354/meps09506>
- 695 Le Hir, P., Cann, P., Waeles, B., Jestin, H., Bassoullet, P., 2008. Chapter 11 Erodibility of natural  
696 sediments: experiments on sand/mud mixtures from laboratory and field erosion tests, in:  
697 Kusuda, T., Yamanishi, H., Spearman, J., Gailani, J.Z. (Eds.), *Proceedings in Marine Science,*  
698 *Sediment and Ecohydraulics*. Elsevier, pp. 137–153. [https://doi.org/10.1016/S1568-](https://doi.org/10.1016/S1568-2692(08)80013-7)  
699 [2692\(08\)80013-7](https://doi.org/10.1016/S1568-2692(08)80013-7)
- 700 Le Hir, P., Monbet, Y., Orvain, F., 2007. Sediment erodability in sediment transport modelling: Can we  
701 account for biota effects? *Cont. Shelf Res., Natural Coastal Mechanisms - Flume and Field*  
702 *Experiments on Links between Biology, Sediments and Flow* 27, 1116–1142.  
703 <https://doi.org/10.1016/j.csr.2005.11.016>
- 704 Lehuen, A., Orvain, F., 2024. A cockle-induced bioturbation model and its impact on sediment erodibility:  
705 A meta-analysis. *Sci. Total Environ.* 912, 168936.  
706 <https://doi.org/10.1016/j.scitotenv.2023.168936>
- 707 Lenth, R.V., Bolker, B., Buerkner, P., Giné-Vázquez, I., Herve, M., Jung, M., Love, J., Miguez, F., Riebl,  
708 H., Singmann, H., 2023. emmeans: Estimated Marginal Means, aka Least-Squares Means.
- 709 Li, B., Cozzoli, F., Soissons, L.M., Bouma, T.J., Chen, L., 2017. Effects of bioturbation on the erodibility  
710 of cohesive versus non-cohesive sediments along a current-velocity gradient: A case study on  
711 cockles. *J. Exp. Mar. Biol. Ecol.* 496, 84–90. <https://doi.org/10.1016/j.jembe.2017.08.002>
- 712 Louters, T., Van den Berg, J.H., Mulder, J.P.M., 1998. Geomorphological changes of the Oosterschelde  
713 tidal system during and after the implementation of the Delta project. *J. Coast. Res.* 14, 1134–  
714 1151.
- 715 Lüdecke, D., Ben-Shachar, M.S., Patil, I., Waggoner, P., Makowski, D., 2021. performance: An R  
716 Package for Assessment, Comparison and Testing of Statistical Models. *J. Open Source Softw.*  
717 6, 3139. <https://doi.org/10.21105/joss.03139>
- 718 Meysman, F.J.R., Middelburg, J., Heip, C., 2006. Bioturbation: a fresh look at Darwin's last idea. *Trends*  
719 *Ecol. Evol.* 21, 688–695. <https://doi.org/10.1016/j.tree.2006.08.002>
- 720 Montserrat, F., Van Colen, C., Provoost, P., Milla, M., Ponti, M., Van den Meersche, K., Ysebaert, T.,  
721 Herman, P.M.J., 2009. Sediment segregation by biodiffusing bivalves. *Estuar. Coast. Shelf Sci.*  
722 83, 379–391. <https://doi.org/10.1016/j.ecss.2009.04.010>
- 723 Morelle, J., Huguet, A., Richard, A., Laverman, A.M., Roose-Amsaleg, C., Parlanti, E., Sourzac, M.,  
724 Mesnage, V., Lecoq, N., Deloffre, J., Viollier, E., Maire, O., Orvain, F., 2024. Antagonistic  
725 impacts of benthic bioturbator species: Interconnected effects on sedimentary properties,  
726 biogeochemical variables, and microbial dynamics. *J. Exp. Mar. Biol. Ecol.* 573, 152000.  
727 <https://doi.org/10.1016/j.jembe.2024.152000>
- 728 Orvain, F., 2005. A model of sediment transport under the influence of surface bioturbation:  
729 generalisation to the facultative suspension-feeder *Scrobicularia plana*. *Mar. Ecol. Prog. Ser.*  
730 286, 43–56. <https://doi.org/10.3354/meps286043>
- 731 Orvain, F., De Crignis, M., Guizien, K., Lefebvre, S., Mallet, C., Takahashi, E., Dupuy, C., 2014a. Tidal  
732 and seasonal effects on the short-term temporal patterns of bacteria, microphytobenthos and  
733 exopolymers in natural intertidal biofilms (Brouage, France). *J. Sea Res., Trophic significance*  
734 *of microbial biofilm in tidal flats* 92, 6–18. <https://doi.org/10.1016/j.seares.2014.02.018>
- 735 Orvain, F., Guizien, K., Lefebvre, S., Bréret, M., Dupuy, C., 2014b. Relevance of macrozoobenthic  
736 grazers to understand the dynamic behaviour of sediment erodibility and microphytobenthos  
737 resuspension in sunny summer conditions. *J. Sea Res., Trophic significance of microbial biofilm*  
738 *in tidal flats* 92, 46–55. <https://doi.org/10.1016/j.seares.2014.03.004>

- 739 Orvain, F., Hir, P.L., Sauriau, P.-G., 2003. A model of fluff layer erosion and subsequent bed erosion in  
740 the presence of the bioturbator, *Hydrobia ulvae*. J. Mar. Res. 61, 821–849.  
741 <https://doi.org/10.1357/002224003322981165>
- 742 Orvain, F., Sauriau, P., Sygut, A., Joassard, L., Le Hir, P., 2004. Interacting effects of *Hydrobia ulvae*  
743 bioturbation and microphytobenthos on the erodibility of mudflat sediments. Mar. Ecol. Prog.  
744 Ser. 278, 205–223. <https://doi.org/10.3354/meps278205>
- 745 Orvain, F., Sauriau, P.-G., 2002. Environmental and behavioural factors affecting activity in the intertidal  
746 gastropod *Hydrobia ulvae*. J. Exp. Mar. Biol. Ecol. 272, 191–216. [https://doi.org/10.1016/S0022-0981\(02\)00130-2](https://doi.org/10.1016/S0022-0981(02)00130-2)
- 748 Paarlberg, A.J., Knaapen, M.A.F., de Vries, M.B., Hulscher, S.J.M.H., Wang, Z.B., 2005. Biological  
749 influences on morphology and bed composition of an intertidal flat. Estuar. Coast. Shelf Sci. 64,  
750 577–590. <https://doi.org/10.1016/j.ecss.2005.04.008>
- 751 Passarelli, C., Olivier, F., Paterson, D.M., Meziane, T., Hubas, C., 2014. Organisms as cooperative  
752 ecosystem engineers in intertidal flats. J. Sea Res., Trophic significance of microbial biofilm in  
753 tidal flats 92, 92–101. <https://doi.org/10.1016/j.seares.2013.07.010>
- 754 Posfai, A., Taillefumier, T., Wingreen, N.S., 2017. Metabolic Trade-Offs Promote Diversity in a Model  
755 Ecosystem. Phys. Rev. Lett. 118, 028103. <https://doi.org/10.1103/PhysRevLett.118.028103>
- 756 Rakotomalala, C., Grangeré, K., Ubertini, M., Forêt, M., Orvain, F., 2015. Modelling the effect of  
757 *Cerastoderma edule* bioturbation on microphytobenthos resuspension towards the planktonic  
758 food web of estuarine ecosystem. Ecol. Model. 316, 155–167.  
759 <https://doi.org/10.1016/j.ecolmodel.2015.08.010>
- 760 Robinson, D., Hayes, A., Couch, S., 2023. broom: Convert Statistical Objects into Tidy Tibbles [WWW  
761 Document]. URL <https://github.com/tidymodels/broom> (accessed 2.26.24).
- 762 Soares, C., Sobral, P., 2009. Density-dependent effects of bioturbation by the clam, *Scrobicularia plana*,  
763 on the erodibility of estuarine sediments. Mar. Freshw. Res. 60, 737–744.  
764 <https://doi.org/10.1071/MF08069>
- 765 Thrush, S., Hewitt, J., Norkko, A., Nicholls, P., Funnell, G., Ellis, J., 2003. Habitat change in estuaries:  
766 predicting broad-scale responses of intertidal macrofauna to sediment mud content. Mar. Ecol.  
767 Prog. Ser. 263, 101–112. <https://doi.org/10.3354/meps263101>
- 768 van Prooijen, B.C., Montserrat, F., Herman, P.M.J., 2011. A process-based model for erosion of  
769 *Macoma balthica*-affected mud beds. Cont. Shelf Res. 31, 527–538.  
770 <https://doi.org/10.1016/j.csr.2010.12.008>
- 771 Widdows, J., Brinsley, M., 2002. Impact of biotic and abiotic processes on sediment dynamics and the  
772 consequences to the structure and functioning of the intertidal zone. J. Sea Res., Structuring  
773 Factors of Shallow Marine Coastal Communities, Part I 48, 143–156.  
774 [https://doi.org/10.1016/S1385-1101\(02\)00148-X](https://doi.org/10.1016/S1385-1101(02)00148-X)
- 775 Widdows, J., Brinsley, M.D., Bowley, N., Barrett, C., 1998. A Benthic Annular Flume for In Situ  
776 Measurement of Suspension Feeding/Biodeposition Rates and Erosion Potential of Intertidal  
777 Cohesive Sediments. Estuar. Coast. Shelf Sci. 46, 27–38.  
778 <https://doi.org/10.1006/ecss.1997.0259>
- 779 Widdows, V., Brown, S., Brinsley, M.D., Salkeld, P.N., Elliott, M., 2000. Temporal changes in intertidal  
780 sediment erodability: influence of biological and climatic factors. Cont. Shelf Res. 20, 1275–  
781 1289. [https://doi.org/10.1016/S0278-4343\(00\)00023-6](https://doi.org/10.1016/S0278-4343(00)00023-6)
- 782 Willows, R.I., Widdows, J., Wood, R.G., 1998. Influence of an infaunal bivalve on the erosion of an  
783 intertidal cohesive sediment: A flume and modeling study. Limnol. Oceanogr. 43, 1332–1343.  
784 <https://doi.org/10.4319/lo.1998.43.6.1332>
- 785 Ysebaert, T., Herman, P.M.J., Meire, P., Craeymeersch, J., Verbeek, H., Heip, C.H.R., 2003. Large-  
786 scale spatial patterns in estuaries: estuarine macrobenthic communities in the Schelde estuary,  
787 NW Europe. Estuar. Coast. Shelf Sci. 57, 335–355. [https://doi.org/10.1016/S0272-7714\(02\)00359-1](https://doi.org/10.1016/S0272-7714(02)00359-1)
- 789 Zhou, Z., 2023. Benthic macrofauna under extremes: Unravelling the response strategies from  
790 individual behaviour to community structure in tidal flats. NIOZ Royal Netherlands Institute for

791 Sea Research, Department of Estuarine and Delta Systems, Utrecht University, Yerseke, The  
792 Netherlands Faculty of Geosciences, Department of Physical Geography, Utrecht University,  
793 The Netherlands, Yerseke.  
794

## 795 Reference list

796 Figure 1 A: Fauna models used in their sediment. B: Classification of species according to the  
797 different effects of bioturbation on sediment characteristics (references in Supplementary data 2.1,  
798 SuppFig 2.B and SuppTab 2.C).

799 Figure 2 Maps of sampling location for each species and sediment.

800 Figure 3 A: Experimental design. B: Measurement's chronology. LT: low tide, HT: high tide, O<sub>2</sub>:  
801 respiration chamber, pot: incubation core, sample: sample bearer for the erosion flume, ERIS: erosion  
802 flume. The green frame represents the steps with a controlled temperature. C: Mesocosms tidal rhythm  
803 for each duo. The blue arrow represents the respiration measurement and the installation in the pot, the  
804 red arrow the bioturbation phase, the red dotted line the holding period of *C. volutator* and *P. ulvae* in a  
805 dedicated mesocosm prior to installation on sample bearer.

806 Figure 4 A:  $Itot_{respi}$  [mW.m<sup>-2</sup>] vs  $Itot_{meso}$ , with standard deviation and its regression line for each duo  
807 (corresponding colours) and in grey for all data combined, the grey dotted line represents the identity  
808 relation. Note that the scales are Box-Cox transformed, and the regression lines were made on  
809 transformed data. B: ANCOVA results for  $Itot_{respi}$  transformed  $\sim$   $Itot_{meso}$  transformed + Duo +  
810 Temperature. Filled dot are p-value  $\leq$  0.1 and empty dot are p-value  $>$  0.1.

811 Figure 5 Erosion  $M_{erod}$  (g.m<sup>-2</sup>) vs time (s) and mesocosm metabolic rate ( $Itot_{meso}$  [mW.m<sup>-2</sup>]). The thick  
812 solid lines represent the steps identified as mass erosion steps. The various colours represent the  
813 different combination of species and temperature.

814 Figure 6 Fluff layer quantity ( $Q_{fluff}$  [g.m<sup>-2</sup>]) vs the different metabolic rate evaluation [mW.m<sup>-2</sup>]: based  
815 on the measured respiration rate  $Itot_{respi}$  (A), the  $Itot$  with the mesocosm temperature  $Itot_{meso}$  (B) and the  
816  $Itot$  with the flume temperature  $Itot_{flume}$  (C) and their regression line. Note that the y scale is Box-Cox  
817 transformed, and the models were made on transformed data.

818 Figure 7 Right column: results for transformed  $Q_{fluff}$  - A1) ANCOVA model using the temperature as  
819 factor and the  $Itot_{meso}$  as covariant; A2) ANCOVA model using the duos as factor and the  $Itot_{meso}$  as  
820 covariant; Left column: results for transformed  $BSS_{mass}$  - B1) ANCOVA model using the temperature as  
821 factor and the  $Itot_{meso}$  as covariant; B2) ANCOVA model using the duos as factor and the  $Itot_{meso}$  as  
822 covariant. Filled dot are p-value  $\leq$  0.1 and empty dot are p-value  $>$  0.1.

823 Figure 8 Critical bed shear stress ( $BSS_{mass}$  [Pa]) vs the different metabolic rate evaluation [mW.m<sup>-2</sup>]:  
824 the measured respiration rate  $Itot_{respi}$  (A), the  $Itot$  with the mesocosm temperature  $Itot_{meso}$  (B) and the  $Itot$   
825 with the flume temperature  $Itot_{flume}$  (C) and their regression line. Note that the scales are Box-Cox  
826 transformed, and the models were made on transformed data.

827

828 **Table list**

829        Table 1 Linear regression estimates for each species  $I_{tot_{meso}}$  ( $y = \text{Intercept} + \beta_{S1} \cdot S1 + \beta_{S2} \cdot S2$ ), with  
830 95% confidence interval in all experiments and by duos separated for  $Q_{fluff}$  and  $BSS_{mass}$ .

831